EVREST Project Report:

Synthetic report on geomorphological evolution of the study sites

Project Funding: Fundação para a Ciência e a Tecnologia (FCT)

Scientific Domain: Marine Sciences and Earth Sciences - Estuarine Coastal and Littoral Systems

Project reference: PTDC/MAREST/1031/2014

Report Title	Synthetic report on geomorphological evolution of the study sites
Reporting Period	01/05/2017-31/02/2018
Authors	Katerina Kombiadou & Ana Matias
Delivery Date	30/04/2018
Related Task	Task 3: Analysis of geomorphological evolution
Objective	To quantify evolution rates, to identify resilient environments, to identify differences on environments resilience, and to compare datasets covering different timeframes
Coordinators	Óscar Ferreira & Ana Matias
Participants	Rita Carrasco, Rui Taborda, Theocharis Plomaritis & Katerina Kombiadou

TABLE OF CONTENTS

TABLE OF FIGURES

TABLE OF TABLES

1. INTRODUCTION

The present report refers to the activities performed under Task 3 of the EVREST project, regarding the mapping of coastlines and boundaries of distinct geomorphological units in Ria Formosa, based on the raster datasets collected. The geomorphological evolution is analysed based on linear regression rates of the digitised boundaries and on the long and short-term temporal evolution of the selected geomorphological units and transects along the barrier.

The three geomorphological units include:

- **Barrier:** corresponds to the wave dominated part of the barrier
- **Dune:** corresponds to the wind dominated part of the barrier
- **Marsh:** corresponds to the tide dominated part of the backbarrier

The boundaries of the geomorphological units digitised include:

- Ocean-side:
    - ⮥ **Wet-dry line:** corresponds to the Mean Water Level (MWL) at the time of the flight
    - ⮥ **Debris line:** corresponds to the Mean High Water Level (MHWL) at the time of the flight
    - ⮥ **Dune line:** corresponds to the foredune foot (edge of dune vegetation) and to ca. the Mean Highest High Water Level (MHHWL)
- Lagoon-side:
    - ⮥ **Backbarrier line:** corresponds to the MHWL in the lagoon side
    - ⮥ **Marsh edge:** corresponds to the limit between marsh vegetation and tidal flat (ca. MWL)

The analysis is performed on all the barriers of Ria Formosa. A map of the study area, showing the location of the 7 barriers and the 6 inlets (current configuration) is given in Figure 1.
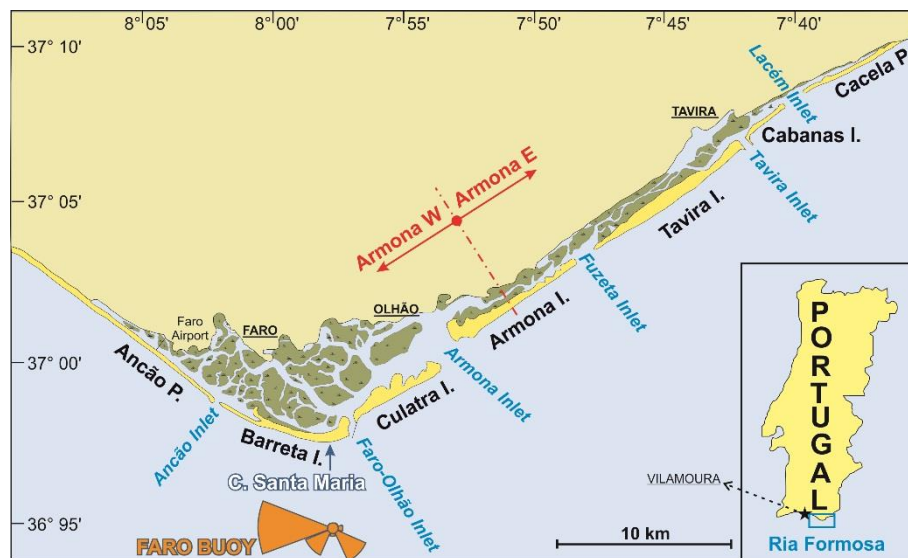
Figure 1: The Ria Formosa barrier island system; the location of the Faro buoy and the Santa Maria Cape are noted on the map, as well as the names of islands, peninsulas, inlets and the division of Armona to W and E.

2. DATA AND METHODS

2.1 Data availability and spatial-temporal coverage

The basis for the digitisation process is the raster datasets collected and processed under Task 1 (Data collection and GIS integration). More on the data processing can be found in the related report (Kombiadou & Matias, 2017).

The coverage of the seven barriers of Ria Formosa (Figure 1) in the available aerial photography is given in Table 1. Given that the evolution of Cabanas Island and Cacela Peninsula is interlinked, there barriers are referred to in a joined manner, as the Cabanas-Cacela subsystem. The boundaries of the selected geomorphological units were mapped in all the available imagery.
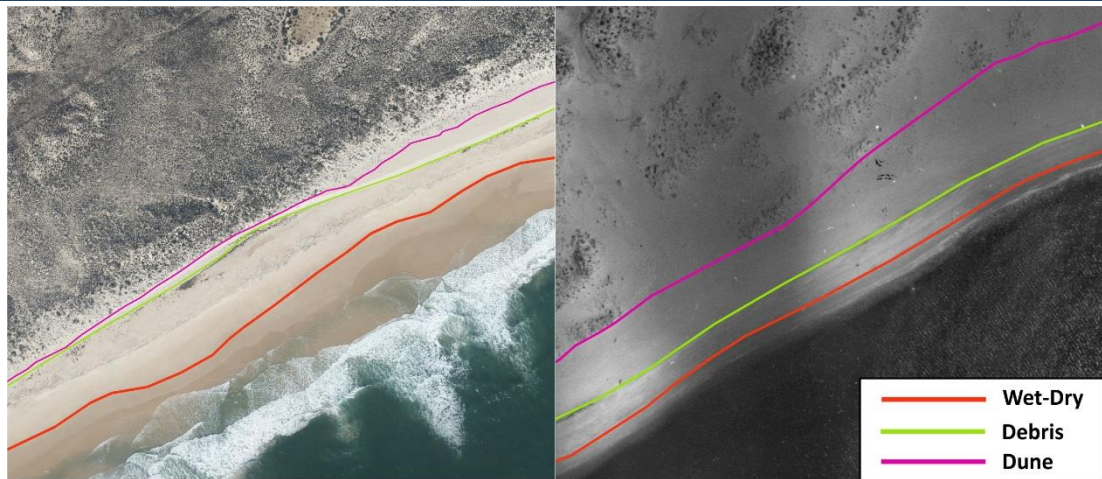
Table 1: Barrier coverage from the compiled raster dataset.

year	Ancão	Barreta	Culatra	Armona	Tavira	Cabanas-Cacela
2014	full	full	full	full	full	full
2009	full	full	full	full	none	none
2008	full	full	full	full	full	full
2005	full	full	full	full	full	full
2002	full	full	full	full	full	full
2001	full	full	full	full	full	full
2000	none	full	full	full	full	none
1999	full	full	full	full	full	none
1996	full	full	full	full	full	full
1989	full	full	full	partial	full	full
1986	none	partial	partial	none	partial	full
1985	full	full	full	full	full	full
1980	full	full	full	full	full	full
1976	full	full	full	full	full	full
1972	full	full	full	full	full	partial
1969	partial	none	partial	full	full	partial
1958	full	full	full	full	full	full
1952	full	full	full	full	full	full
1947	full	full	full	full	full	full

2.2 Shoreline mapping criteria

The criteria used for the visual identification of the boundaries between geomorphological units in the raster datasets are summarised in Table 2. The boundary lines were mapped using all the available raster datasets and using a common geographical system (GCS Datum 73 IGeoE).

Table 2: Criteria used for the visual identification and digitisation of the boundary lines in the ocean and the lagoon side, along with examples for colour (left) and grayscale photos (right).

	Wet-Dry	Dune	Debris
Ocean-side boundary lines	Sand colour transition from dark to clear	Edge of dune vegetation	If debris present, the upper limit of debris, if not, the beach scarp.

	Backbarrier	Marsh edge
Lagoon-side	If vegetated, transition to bushy (more rugose, darker) vegetation, if not, dune limit or debris line.	Transition to tidal flat: if vegetated, boundary between emergent and submerged vegetation (colour, texture), if not, edge of tidal channel.

An example of the digitised wet-dry and backbarrier lines, in the ocean and lagoon side respectively, for Culatra Island is given in Figure 2. The transition from the oldest to the most recent flights (1947 to 2014) is denoted with a colour transition of blue-green-yellow-red, as shown in the figure legend.
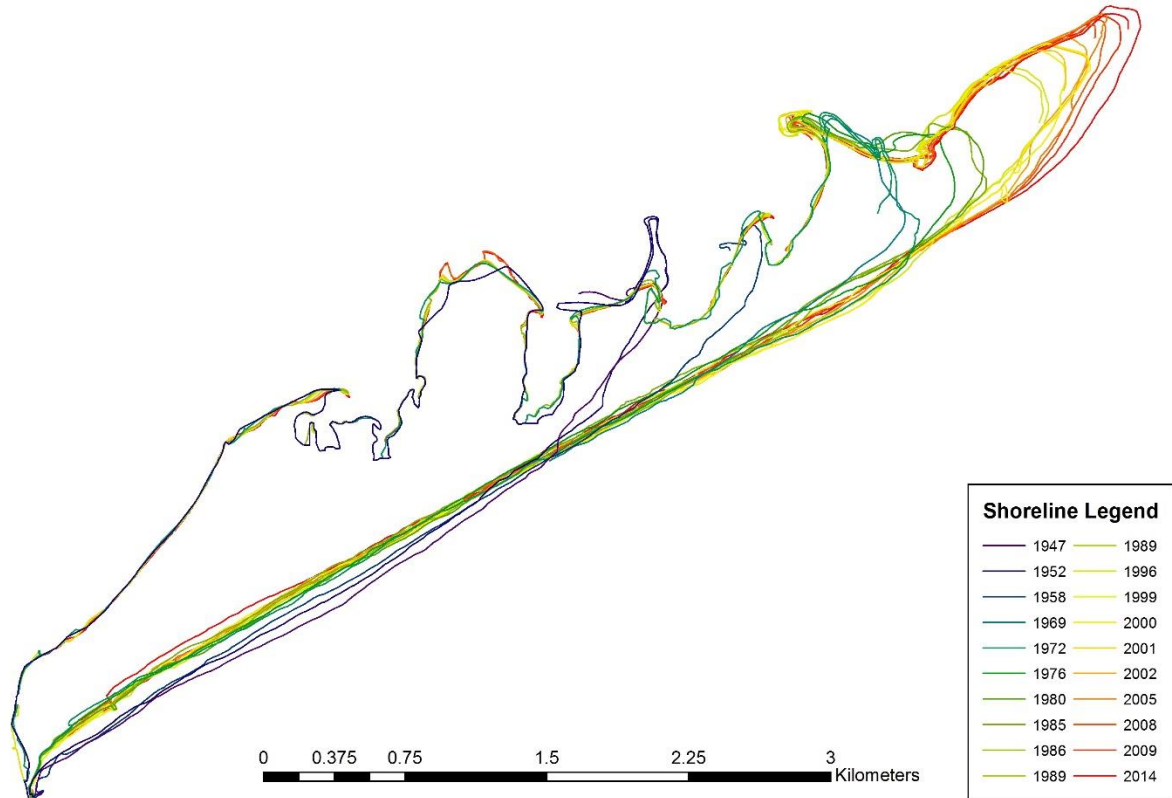
Figure 2: Example of the digitised ocean-side shoreline (wet-dry) and the lagoon-side backbarrier line for Culatra Island and all the available flights (colour coding is denoted on the legend).

2.3 Shoreline analysis

2.3.1 Spatio-temporal scales

The lines were analysed in terms of long-term (multi-decadal) and short-term (years to decades) evolution, as well as for each barrier as a whole and examining the evolution of distinct areas of the barrier that exhibit similar development. To that aim, two rates of change were quantified:

- ➲ **Linear regression rates:** correspond to the rates of change of each boundary line with time (defined in m/yr).
- ➲ **Barrier areas:** correspond to the total area of each geomorphological unit analysed or its' relative changes in time (defined in m^2 or m^2/yr).

2.3.2 Shoreline regression rates

The assessment of shoreline regression rates was performed using the Digital Shoreline Analysis (DSAS) tool (Thieler, Himmelstoss, Zichichi, & Ergul, 2009). The tool defines the shoreline changes along transects that are cast perpendicular to a reference baseline (user-defined spacing between transects and position and morphology of the baseline). An example for the morphology of the baseline and transects used by DSAS for the dune line of Ancão, as well as the calculation of temporal evolution of shoreline position changes with time by the position of intersection with the transects, is shown in Figure 3.

4
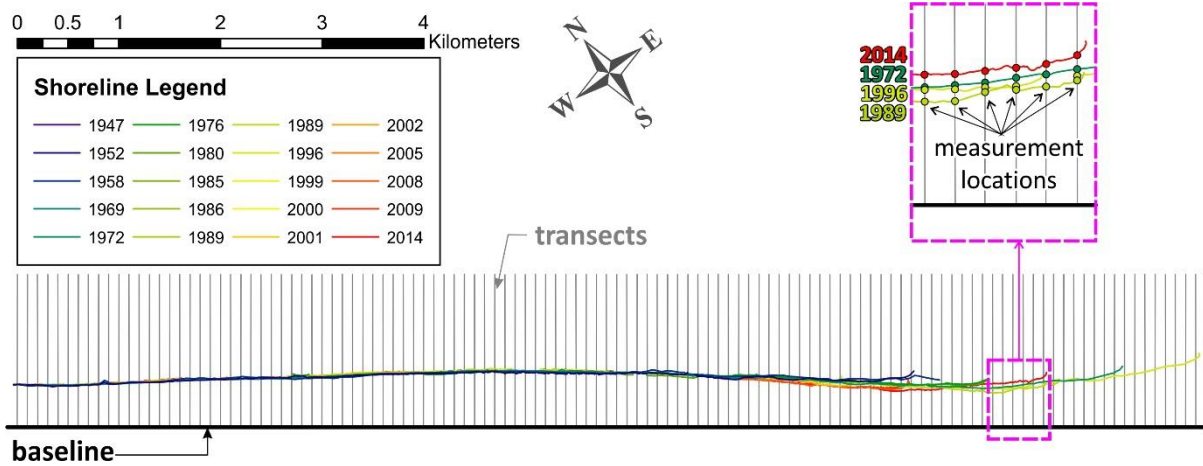
Figure 3: Indicative representation of the baseline and transects used for the determination of shoreline regression rates; the boundary lines shown correspond to the Ancão dune line and the magnified area (in pink dashed rectangle) shows the intersection of transects and shorelines used as measurement locations by DSAS.

The metrics, calculated by DSAS, and provided as output include:

Distance measurements:

- Shoreline Change Envelope
- Net Shoreline Movement

Statistics:

- End Point Rate
- Least Squares Regression
- Weighted Least Squares Regression
- Supplemental statistics for Least and Weighted regression
- Confidence Interval
- Standard Error
- R-squared

The analysis performed within EVREST is based on Weighted Least Squares Regression and the calculation of Weighted Linear Regression (WLR) rates. The WLR is similar to the Linear Regression Rate (LRR), however, the regression process adds more weight towards data with greater certainty, thereby weighting the change rate toward more accurate shoreline positions (Terrano, Flocks, & Smith, 2016).

To perform a weighted least squares regression, the **uncertainty** associated with each shoreline needs to be quantified. The process used for the assessment of uncertainty values is described in the following subsection.

2.3.3 Uncertainty assessment of boundary lines

The total shoreline position error can be assessed as the sum of squares of all measurement errors, which, in a general form, can be written as (Morton, Miller, & Moore, 2004):

$$\mathrm{E}_{sp} = \sqrt{E_r^2 + E_d^2 + E_t^2 + E_o^2 + E_l^2} \qquad [1]$$

These errors include the rectification error (E_r), the digitizing error (E_d), the T-sheet survey error (E_t), the shoreline proxy offset (E_o) and the Lidar position error (E_l). From these errors, E_t pertains only to

the T-survey related shorelines, E_o refers to maximum horizontal offset between high-water and mean high-water shorelines in the Southeast Atlantic region (pertains only to Lidar-derived shorelines) and E_l is the maximum error associated with the derivation of a Lidar shoreline. Therefore, these three errors do not pertain for the case of shorelines derived from digitisation on aerial photographs and equation 1 can be simplified to:

$$\mathrm{E}_{sp} = \sqrt{E_r^2 + E_d^2}$$ [2]

The rectification error (E_r) was taken equal to the accumulated RMSE, that corresponds the total error associated with the backwards-in-time georeferencing process (Kombiadou & Matias, 2017). The digitizing error (E_d) refers to the error associated with the shoreline mapping process; it was taken equal to four times the raster cell size, after Jabaloy-Sánchez et al. (2014), who ascertain that:

> *"Assuming that orthophotographs present an integrated error lower than pixel resolution (1 m), coastlines obtained through digitalization will present errors in the range of 4–8 m (pixel neighbourhood) since the digitalization process was made at a scale larger than the pixel display resolution."*

Therefore, the uncertainty of each boundary line was calculated as the sum of squares of the accumulated RMSE and of the quadruple of the raster cell size. Based on this analysis, the uncertainty related with each flight and each barrier is shown in Figure 4. It is noted that flights from 2002 onwards are orthophotographs and, thus, the uncertainty depends only on the digitizing error; this is why the uncertainty is uniform for all barriers, given that it depends only on the image cell size.
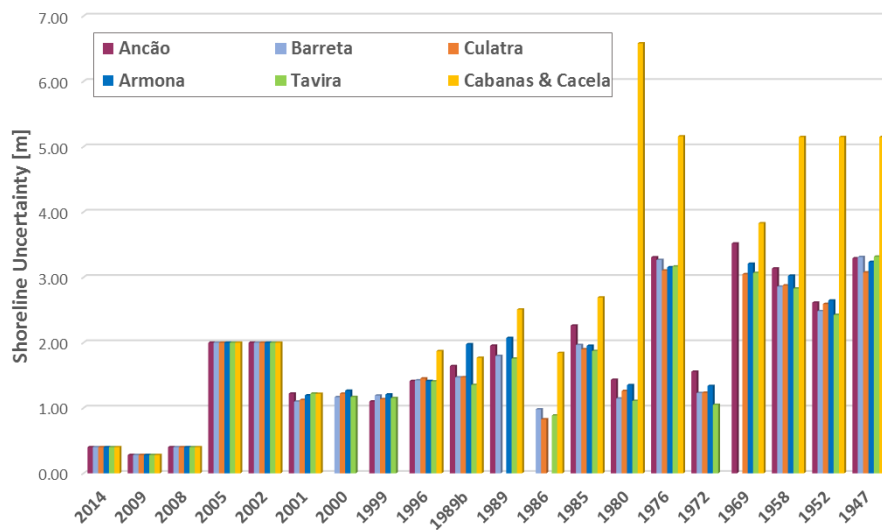
Figure 4: Uncertainty values for all flights and barriers.

2.4 Assessment of Geomorphological Units' Area

The digitised boundaries were used to define polygons for the three geomorphological units under analysis, aiming at calculating the area of each polygon. More specifically, the following polygons were defined:

- **Barrier Island** - wave dominated part of the barrier: delimited by the <u>debris line</u> in the ocean-side and the <u>backbarrier line</u> in the lagoon-side. Both limits correspond to the same water level (ca. MHWL).
- **Dune** - wind dominated part of the barrier: delimited by the <u>dune line</u> in the ocean-side and the <u>backbarrier line</u> in the lagoon-side. The limits correspond to the approximately same water level (ca. MHHWL).
- **Marsh:** - tide dominated part of the backbarrier: delimited by the <u>backbarrier line</u> and the <u>marsh edge line</u> (both in the lagoon-side). These limits correspond to the area between MWL and MHWL.

It is noted that only the flights with full coverage of the barrier were used for the analysis of the area of geomorphological units.

3. Multi-Decadal Weighted Linear Regression (WLR) Rates

The results of the weighted linear regression analysis, calculated for the entire study period (1952 to 2014) are provided in the next parts of the report for all barriers. The barriers are presented from west to east and the WLR rates shown correspond to debris and dune lines in the ocean side and backbarrier and marsh edge for the lagoon side.

3.1 Ancão Peninsula

The results of the long-term morphological analysis of the Ancão Peninsula are shown in Figure 5. The top panel shows the rates of the lagoon-side coastlines and the bottom one the values of the seaward coastlines. To show the main evolution patterns and to facilitate interpretation of WLR rates, indicative digitised coastlines (1952, 1989 and 2014) are also presented.

Figure 5: WLR rates for Ancão Peninsula; the top graph corresponds to lagoon-side boundary lines and the bottom graph to ocean-side ones, while three different barrier morphologies (1952, 1989 and 2014) are also shown.

The evolution of the Ancão Peninsula is dominated by longshore sediment transport and the eastward migration of the Ancão Inlet (Vila-Concejo, Matias, Ferreira, Duarte, & Dias, 2002). As seen in Figure 5, the backbarrier is generaly stable, with low rates of -0.2 to +0.4 m/yr up to a distance of around 7 km along the baseline. Further eastwards, the values present higher variability, ranging from -3 to +2 m/yr, variability that is due to the strong dynamics of the Ancão Inlet. Marsh development is concentrated in the western part of the area, in a zone that extends 4 km eastwards from the connection the peninsula to mainland. The marsh rates are generally low, from -0.6 to +0.5 m/yr and a near-zero average value. In the oceanfront, retreating coastlineline tendencies prevail in the western part and accretive in the eastern, ranging within ±1.0 m/yr for the debris line and between -0.5 to +1.8 m/yr for the dune line; the corresponding average values are -0.3 and +0.2 m/yr. In the inlet-affected eastern part of the barrier the variability increases in both boundaries.

3.2 Barreta Island

In Barreta Island (Figure 6), the beach is dominated by strong progradation, with rates that reach 6 m/yr in the Santa Maria Cape (see location in Figure 1) and range from +2.4 to +3.5 m/yr in the rest

of the coast of the western flank. The southward expansion of the island (maximum shoreline progression of 350 m between 1952 and 2014 at the Cape) is due to the stabilisation of the Faro-Olhão (hereafter F-O) Inlet that enabled the entrapment and accumulation of longshore sediment drift. In the vicinity of the F-O Inlet, erosive tendencies that reach -1.0 m/yr are observed, possibly due to local flow conditions near the western jetty. Localized erosion rates are present in the western area, under the influence of the westward migration of the Ancão Inlet (Vila-Concejo, Matias, Pacheco, Ferreira, & Dias, 2006). In the leeside, the coast is very stable, with near-zero rates, apart from the east and west extremities, the former due to frequent dredging to ensure navigability of the channel and the latter affected by the Ancão inlet migration/closure. The stability of the backbarrier is attributed to the presence of a broad, mature marsh, as also evidenced by the related rates that show a marsh that is either stable, or growing with rates of around 0.5 m/yr that can locally reach 1-5 m/yr.

Figure 6: WLR rates for Barreta Island; the top graph corresponds to lagoon-side boundary lines and the bottom graph to ocean-side ones, while three different barrier morphologies (1952, 1989 and 2014) are also shown.

3.3 Culatra Island

The evolution of Culatra and the related WLR rates are given in Figure 7. Eroding trends exist in the ocean shore of the western part of the island, up to a distance of 3-3.5 km westwards (downdrift) of the F-O Inlet; from there on, the rates become positive with increasing values towards the Armona inlet (~10-20 m/yr). These trends are directly related to the artificial stabilization of the F-O Inlet that produced sediment starvation in the western part and decrease in the tidal prism of the downdrift Armona inlet (Pacheco et al., 2010). The loss of tidal prism resulted to the attachment of the ebb delta shoals to Culatra and accretion of recurved spits in the eastern part of the island (Ferreira, Matias, & Pacheco, 2016). The eastward elongation of the island between 1952 and 2014 is 3 km, corresponding to an average rate of around 50 m/yr, while the peak rates of southward progradation near the

Armona Inlet reach 20 and 25 m/yr for the debris and the dune line, respectively. The results show that there is an apparent clockwise shift of around 5° in the orientation of the island during the study period (the coastline angle was around N 57° E in the 1950s and in the 2010s it reached N 62° E).
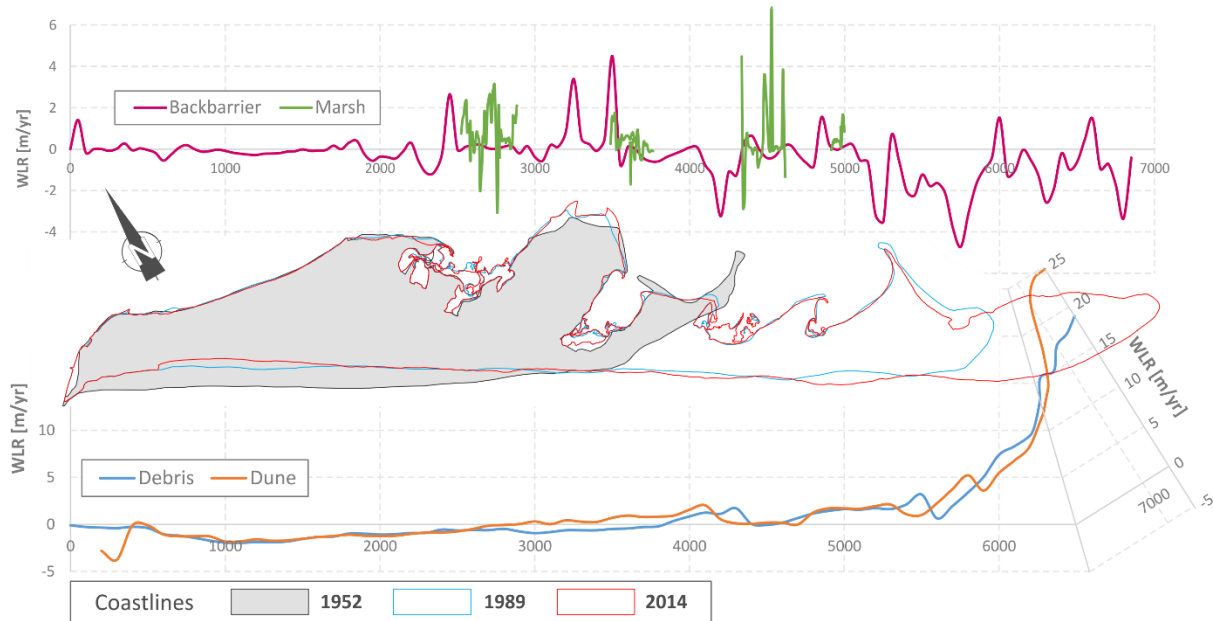
Figure 7: WLR rates for Culatra Island; the top graph corresponds to lagoon-side boundary lines and the bottom graph to ocean-side ones, while three different barrier morphologies (1952, 1989 and 2014) are also shown.

Regarding the evolution in the lagoon side, the backbarrier rates are low in the western, older part of the island (up to 3 km from the inlet), ranging from -1 to +1 m/yr. Eastwards, the values become increasingly variable, ranging from -7.4 to +6.4 m/yr, with an overall average retreat rate of -0.8 m/yr. This variability and dominant retreat tendency is most likely due to the elongation of the island itself, combined with the ebb dominance at the Armona inlet (Ferreira et al., 2016). Regarding marsh evolution, the WLR rates show that the marsh of the west-most, oldest, embayment has been growing since the 1950s with an average rate of +1.0 m/yr. Localised erosive tendencies (-0.6 to -3 m/yr) are most likely due to human pressures (i.e. navigation, shellfish gathering, etc.). This assumption is based on the appearance of geometrical patterns in the marsh vegetation of these areas after marsh-loss incidents. Similar conditions, with marsh development rates around 0.5 to 1.3 m/yr, and low, localised marsh-loss trends, are also observed in the remaining three embayments of the island.

3.4 Armona Island

The WLR rates for Armona Island are given in Figure 8. The results show that the barrier, also impacted by the reduction of the tidal prism in the updrift Armona Inlet, grows towards the NW near the inlet, with average shoreline progradation of 470 m during the study period, significantly lower than the one of Culatra. The related rates in the area are of the order of +5.5 to +15.5 m/yr for both debris and dune lines. These accretive tendencies extend along the ocean side until the middle of the island, with decreasing rates towards the east (average of +0.6 m/yr) and turn erosive near the Fuzeta Inlet, ranging from -0.2 to -1.6 m/yr. The island has an extensive backbarrier and the lagoon-side coastline is stable, apart from the areas near the inlets, where rates can locally reach -6.8 and +9.6 m/yr. The marshes in Armona show general growth in the western part (up to 2 km along the baseline), are near-zero in the central part (around 2 to 4 km along the baseline) and show erosion tendencies of the

order of -2 m/yr to the west (around 4 to 5 km along the baseline). This marsh-loss, as evidenced by the aerial photographs, is probably due to the dredging of the backbarrier channel. Marsh growth is identified near the Fuzeta Inlet, with very high peak values of around +18 m/yr, growth that is due to an artificial embayment, formulated by the disposal of dredged material.
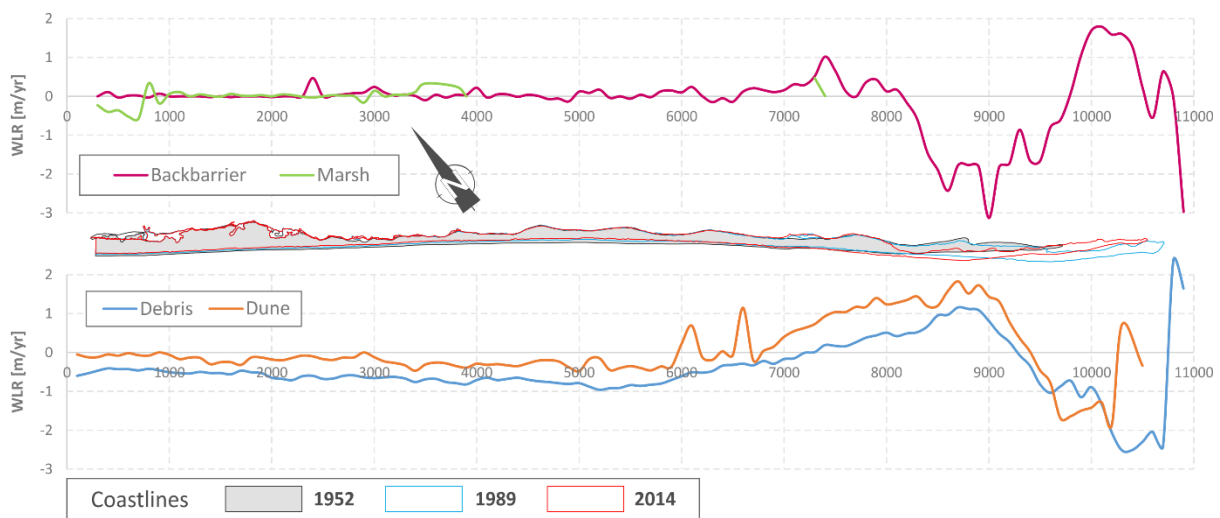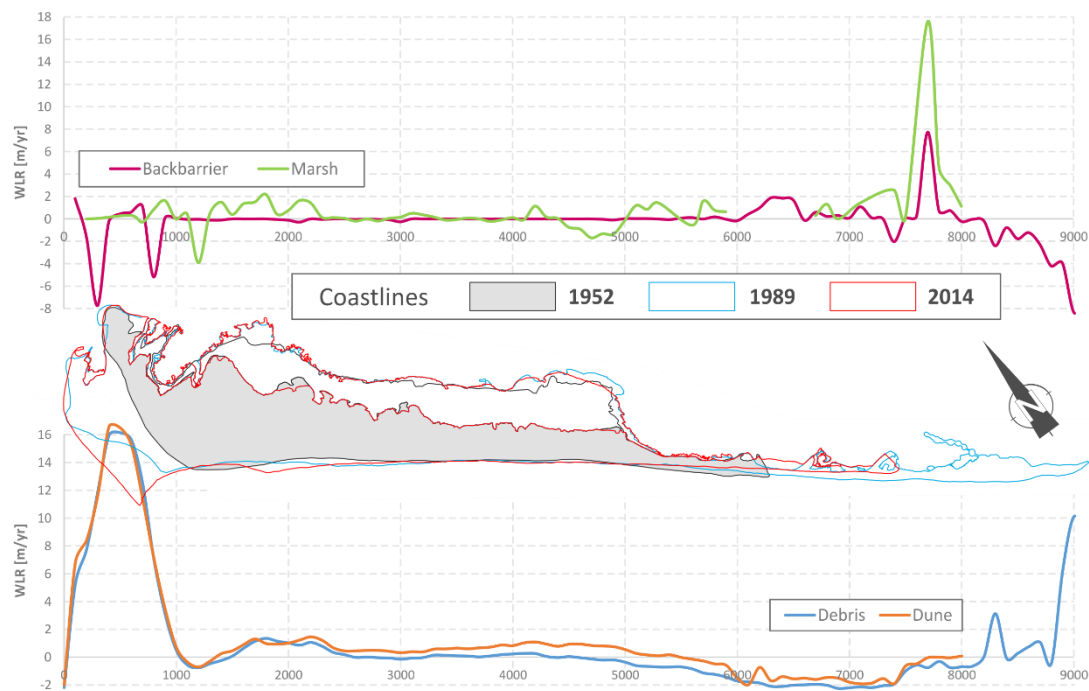

Figure 8: WLR rates for Armona Island; the top graph corresponds to lagoon-side boundary lines and the bottom graph to ocean-side ones, while three different barrier morphologies (1952, 1989 and 2014) are also shown.

3.5 Tavira Island

The WLR rates of Tavira (Figure 9) show that the island presents remarkable stability in the lagoon side during the study period, especially for the backbarrier line (non-zero values near the edges are due to inlet dynamics). The marsh area shows accreting trends, around +0.6 m/yr in the eastern-central part, while for the western part the values are very close to zero. In the oceanfront, both proxies present the same behaviour, with accretion near the Tavira Inlet (up to 3 km from the jetty, updrift), on average by 1.5 m/yr and by a maximum of +4.8 m/yr, and retreat in the central part, with an average rate of -0.8 m/yr. The progradation trends near the Tavira inlet are related with the longshore sediment accumulation against the jetty. As in the case of Culatra, Tavira also shows a clockwise shift in main shoreline orientation during the study period, though significantly lower, of the order of 2° (the coastline angle changed from around N 54° E to N 56° E between 1952 and 2014).
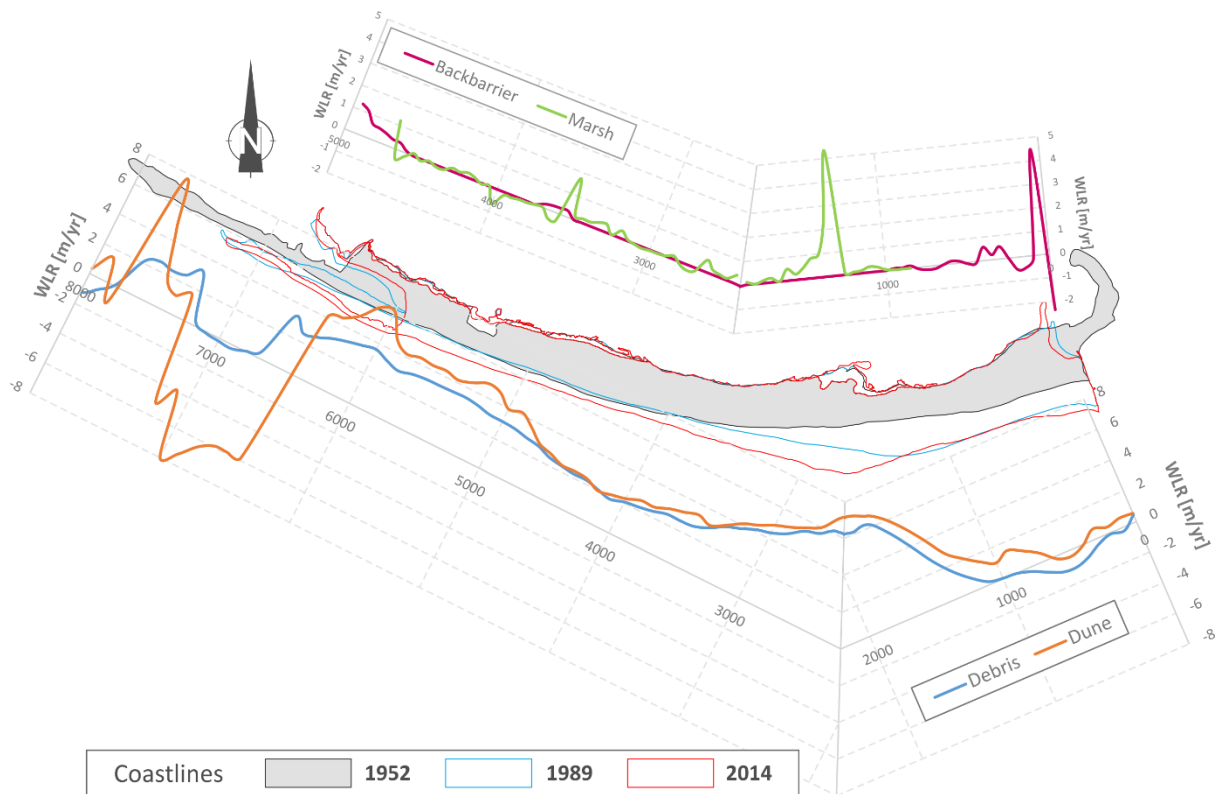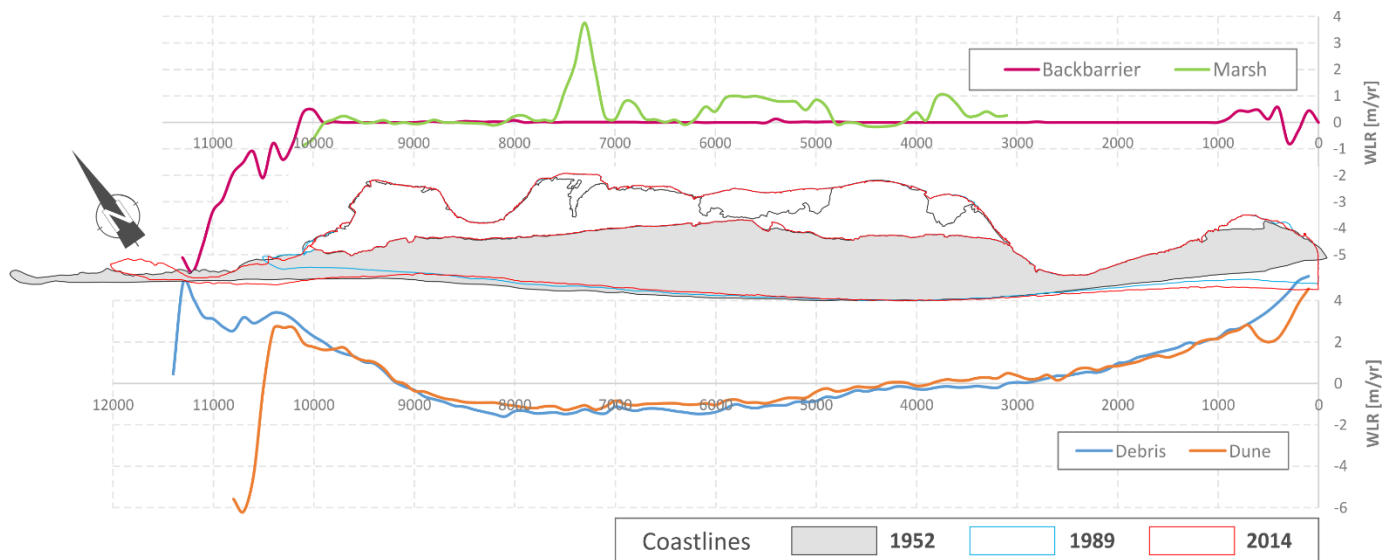
Figure 9: WLR rates for Tavira Island; the top graph corresponds to lagoon-side boundary lines and the bottom graph to ocean-side ones, while three different barrier morphologies (1952, 1989 and 2014) are also shown.

3.6 Cabanas Island – Cacela Peninsula

The results for Cabanas Island and Cacela Peninsula, hereafter referred to as C-C for brevity, are given in Figure 10. Due a shift in the evolution of the island around 1986 (landward migration from 1952 to 1986 and seaward migration from 1986 to 2014), the study period was split in two parts (before and after 1986) and the coastlines were analysed separately within these two temporal windows.

3.6.1 C-C WLR rates for the period of 1952 to 1986

As evidenced by the WLR rates, the entire subsystem presents strong regressive behaviour in the period from 1952 to 1986 (dashed lines in Figure 10). Maximum erosion trends are identified in the central part (2.5 to 6.5 km downdrift from the Tavira jetty) and range from -4 to -14 m/yr, with an average of -7.7 m/yr, for both dune and debris lines. Coastal retreat decreases towards the NE part of C-C due to the attachment of the peninsula to the mainland. In the SW part and up to a distance of 1.5 km east from the Tavira jetty the coastline is largely advancing seawards, due to frequent small-scale nourishment with dredged material from the channel (unrecorded) near the Tavira jetty. The backbarrier is also migrating landwards by an average of 5 m/yr and local maximum rates of 12 m/yr in the central part. The low depths of the backbarrier bay have enabled the transgression of C-C, through frequent overwashes (Matias, Ferreira, Vila-Concejo, Garcia, & Dias, 2008) that move sediment towards the mainland, thus allowing the barriers to shift their position landwards under storm waves. Similarly to the ocean-side coastlines, the high landward migration values of the backbarrier near the Tavira jetty is also due to the unrecorded nourishment in the area. During this period, marshes appear only in the eastern part of C-C, which essentially correspond to the Cacela Peninsula. These marshes show overall growth tendencies, with rates that reach 4.6 m/yr and an average of 0.9 m/yr.
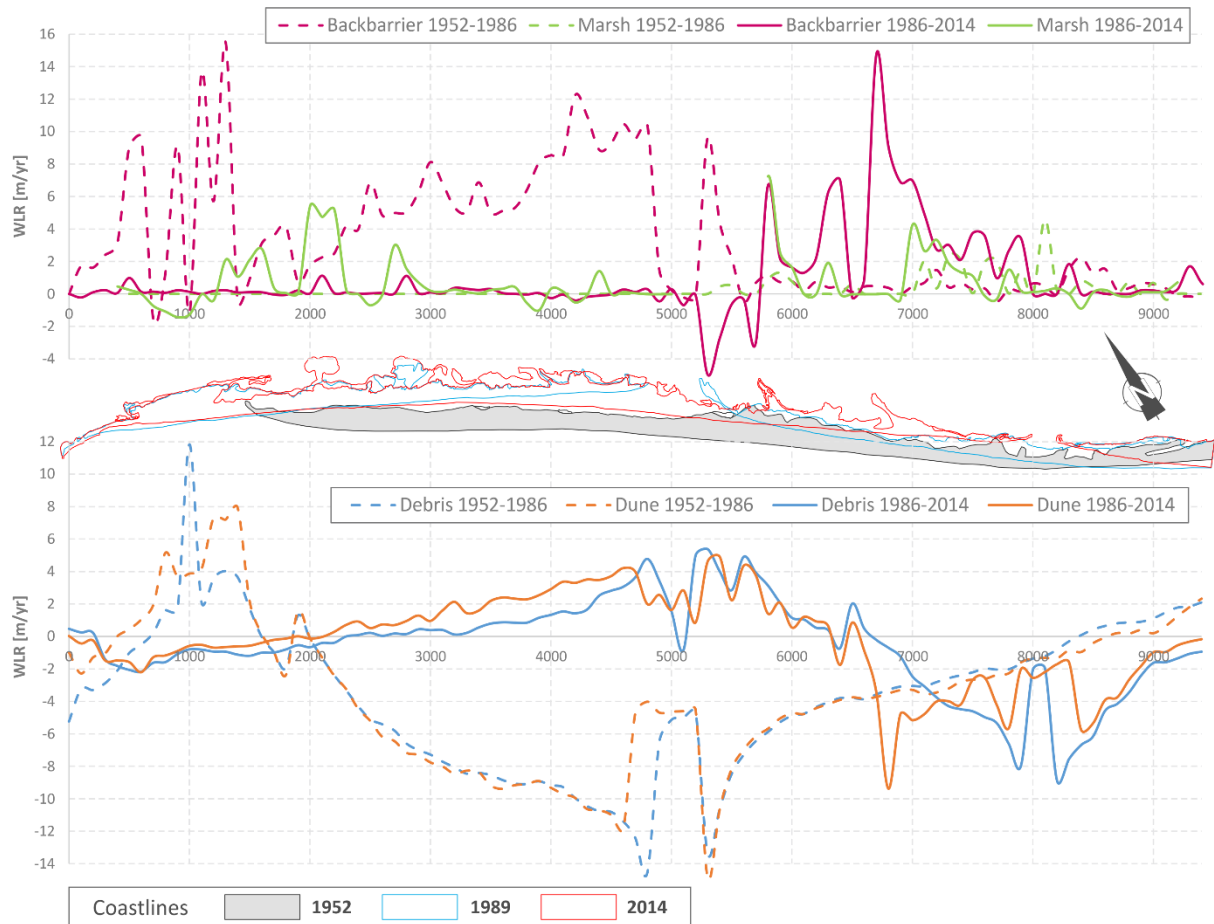
Figure 10: WLR rates for Cabanas Island and Cacela Peninsula; the top graph corresponds to lagoon-side boundary lines and the bottom graph to ocean-side ones, with dashed lines showing the rates from 1952 to 1986 and solid lines the rates from 1986 to 2014. Three different barrier morphologies (1952, 1989 and 2014) are also shown.

3.6.2 C-C WLR rates for the period of 1986 to 2014

In the period from 1986 to 2014 the oceanfront of C-C presents accreting tendencies in the central part (2 to 6.5 km east from the Tavira jetty), for both dune and debris lines, that reach 5 m/yr (with an average of around 2 m/yr). Dune growth in the area is driven by the main washover cessation mechanism, which is berm development along a former breached/inlet (Matias et al., 2008); this results to low foredune development with rapid vertical accretion. In the western part some erosion is evidenced, with peak rates of -2 m/yr. Stronger coastal retreat and dune erosion is present in the eastern part, with maximum erosion rates of -9 m/yr and mean values of -3.2 to -3.6 m/yr.

Regarding marshes, overall, growth or stability can be noted during the period, with peak localised growth values of 3 to 5.5 m/yr and average rates of around 0.8 m/yr. Limited, and mostly localized, erosion rates do not exceed 1.5 m/yr. For the backbarrier, strong stability is noted in the west part (Cabanas Island; zone up to 5 km from the Tavira Inlet), with near-zero values. The remaining part of the area shows higher variability (-5 to +14.7 m/yr), with prevailing retreat tendencies (average of +1.9 m/yr). This variability is due to inlet breaching and the eastward migration of Lacém Inlet, as evidenced by the recent evolution of the barriers, shown in Figure 11. The breaching event of 1995-96 in Cacela P. can be clearly viewed in the top panel of the plot, as well as the eastward migration of the Lacém Inlet and the corresponding eastward elongation of Cabanas Island and the shortening of Cacela Peninsula during this period.
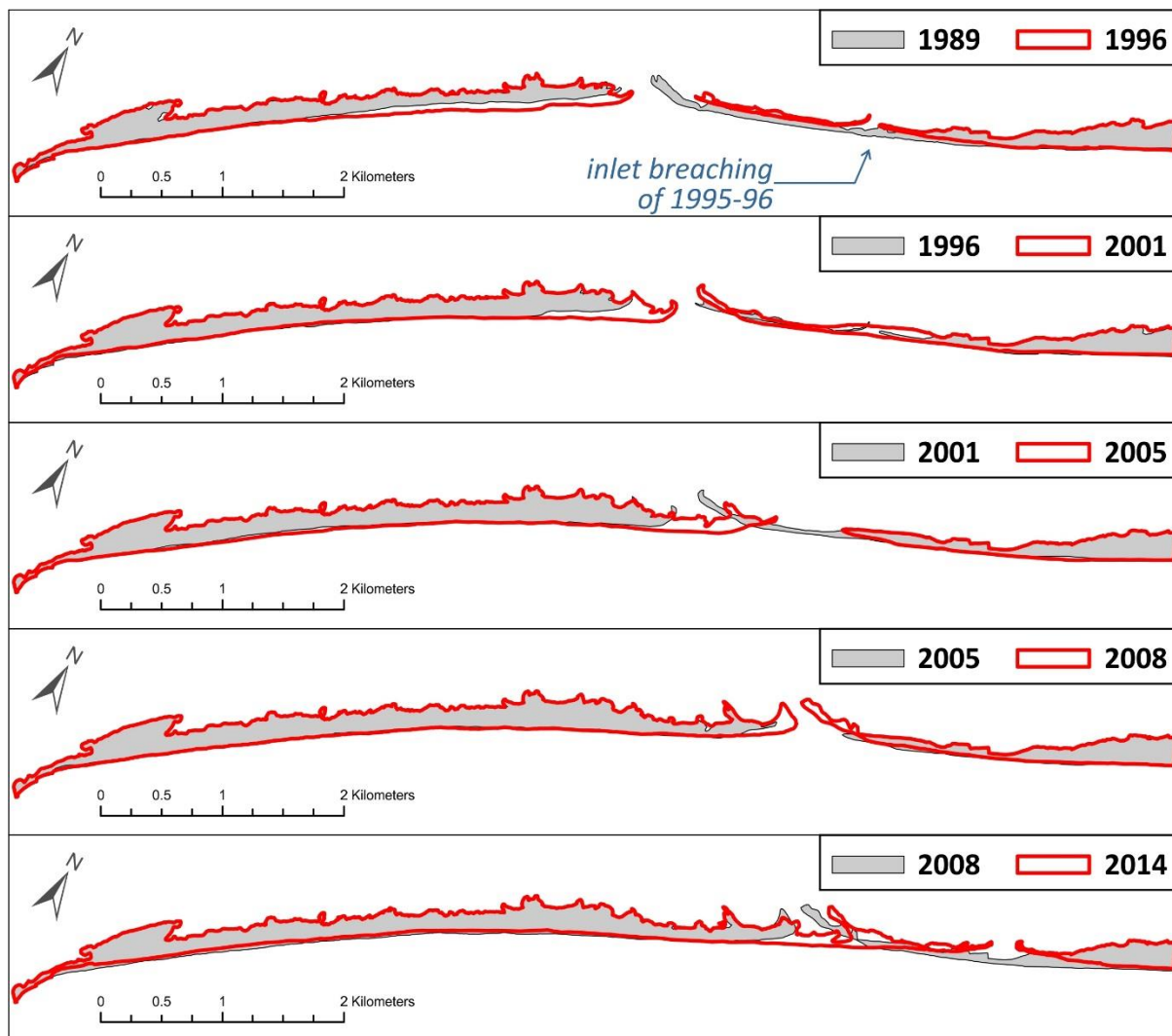
Figure 11: Evolution of the C-C barriers for the period of 1989 to 2014. The panels from top to bottom show successive morphologies of the barrier from two consecutive flights, passing from older to more recent morphologies; the older barrier morphology in each panel is noted as grey-filled area and the newer as red curve.

4. SHORT-TERM EVOLUTION OF GEOMORPHOLOGICAL UNITS

4.1 Short-term evolution – example of Barreta foredune

Apart from the long-term rates defined, the short-term changes in the mapped environments were also analysed. An example of the entire dataset for the dune line in Barreta is shown in Figure 12, where relative change in foredune position is presented for all the transects, uniformly distributed every 100m along the ocean-side baseline (see Figure 6 for position and distances along the baseline). For brevity, the transects are grouped per 5 in each subplot. Thus, the top-left subplot shows the dune evolution for the first 500m along the baseline (transects at 100, 200, 300, 400 & 500m from the F-O jetty), the second subplot (top row) the evolution of the zone from 600 to 1000 m etc.

The results show that up to 1 km W from the F-O Inlet the foredune advances very rapidly until 1972, reaching a progression of 250-300 m in 20 years. From then on, the dune position shows small retreat tendencies, due to local flow conditions, that are responsible for the erosive tendencies in the WLR rates of the area (Figure 6). The area 1.1 to 1.5 km W from the jetty (subplot 3) is a transition zone between the slightly retreating foredunes near the jetty and the area near Cape St. Maria that extends within 1.6 to 3 km along the baseline. This zone (subplots 4, 5 & 7) shows rapid and constant foredune advancement in the area, reaching 400 m between 1958 and 2014. This growth continues along the western flank, with high and quasi-constant rates in the zone between 3.1 and 3.5 km and with lower dune progradation and higher temporal variability in the stretch of 3.6 to 4 km along the baseline. The area from 4.1 to 6 km W from the F-O Inlet (subplots 9-12, 3rd row) shows distinct trends, with small foredune retreat (-20 to -40 m) from 1952 to 1976, followed by rapid growth (~100 m) until 1986 and a period of relative stability, from 1986 to 2000. Recently (since 2005) foredune advance is, once again, noted in the area, reaching 70 m in 9 years. The remaining transects (subplots 13-16, 4th row) refer to the area near the Ancão Inlet, with dune retreat prevailing due to inlet-related processes.
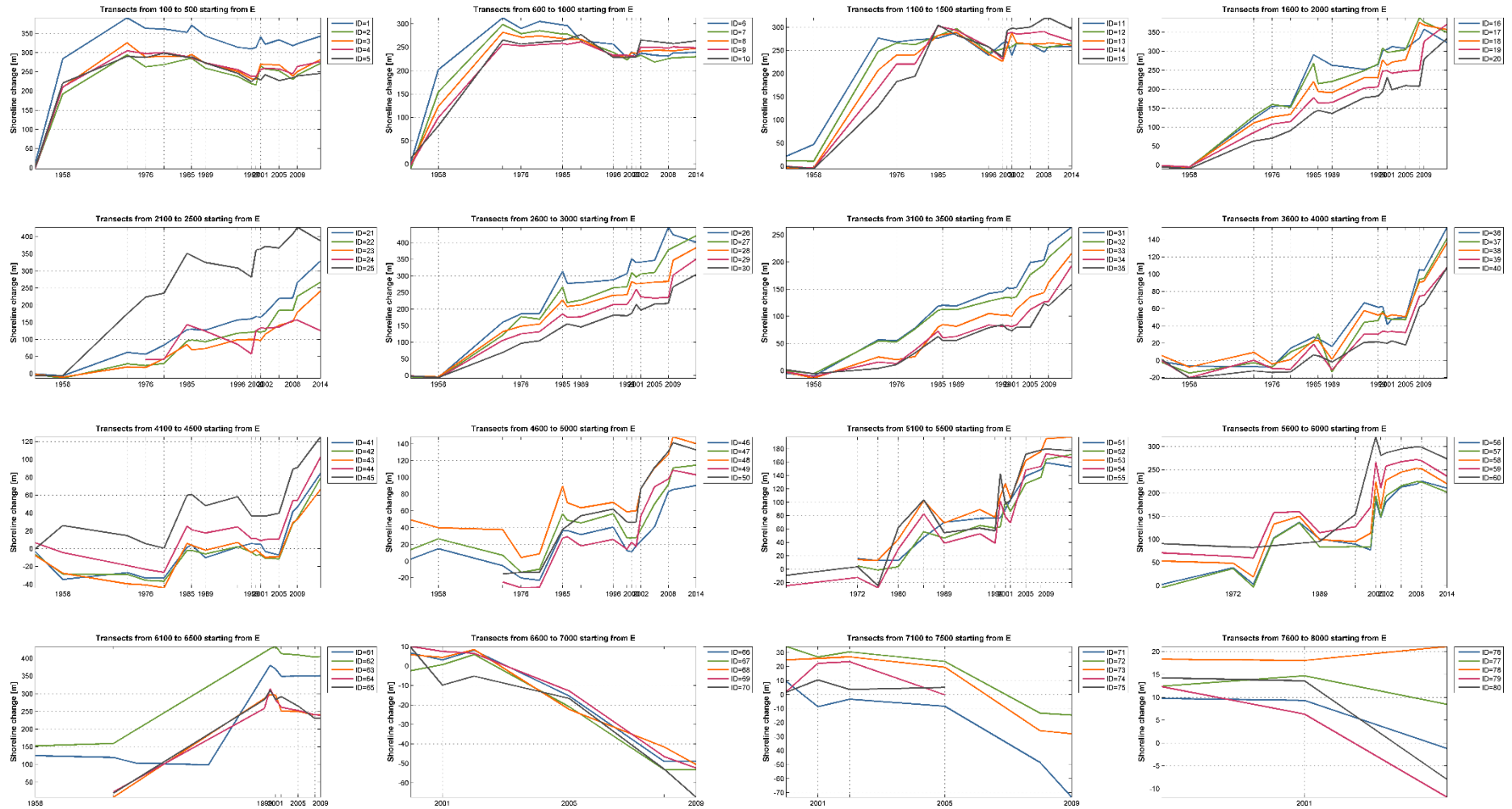
Figure 12: Temporal evolution of relative change in dune position in Barreta Island: Each subplot 5 transects (the ID is given in the legends), starting from E (F-O Inlet) and going to W (Ancão Inlet). The distance between transects is 100m, thus each subplot represents the evolution of 500m along the baseline (see Figure 6 for the position and distances along the baseline).

4.2 Analysis of short-term evolution of morphological units

4.2.1 Methodology

To analyse the short term evolution of the three morphological units under investigation, namely the wave and wind affected parts of the barrier and the marshes, transects were cast along a baseline, common for all boundary limits. Using DSAS, the intersection of transects and boundary lines was determined for all coastlines.

Based on the position of the intersections, the **width of each environmental unit** was determined, as follows:

- **Barrier** (wave-dominated part of the barrier): length of transect between backbarrier and debris line, shown as example in Figure 13
- **Dune** (wind dominated part of the barrier): length of transect between backbarrier and dune line
- **Marsh** (tide dominated part of the backbarrier): length of transect between backbarrier and marsh-edge line

Regarding the position of each of the analysed segments, it was determined as the distance of the centroid of each segment from the baseline (Figure 13). An exception was made for the case of C-C, a barrier very close to the mainland and that exhibited rollover behaviour up to the 1980s; instead of distance from the baseline, the distance from the mainland (digitised coastline) was calculated as the segment position (distance of segment's centroid with the intersection of the transect with the mainland coastline).
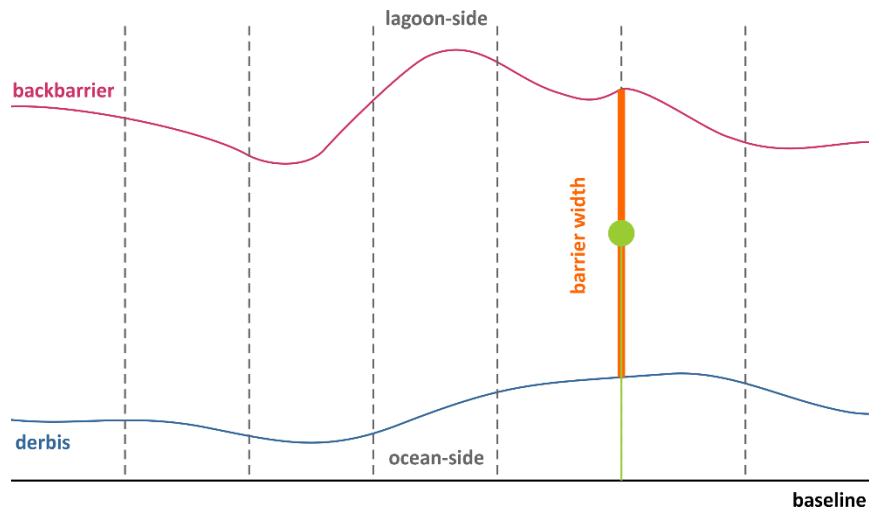
Figure 13: Schematic representation for the calculation of the width and position of an environmental unit, using barrier as an example. The barrier width (orange line) is defined and as the part of the transect (dashed-grey line) delimited by its intersection with the debris and backbarrier lines and the position (green line) is defined as the distance of the centroid of the width (green point) from the baseline.

The selected distance between transects is 100 m. The impact of the selected transect spacing to the quality of the results was tested by comparing the results from two analyses, one using the step of 100 m and one with a fivefold decrease of the spacing (20 m). The results were compared for C-C, barrier selected due to its high spatio-temporal variability, showing that the differences in calculated widths and distances of environmental units was negligible (below 3%). Thus, the barriers, depending on their size, were analysed in 73 to 110 transects. Given the large number of transects, visual

inspection and interpretation of all of them would be nearly impossible. To assist the analysis, the calculated widths and distances from the baseline (or the mainland for C-C) were averaged over 500 m along the baseline (essentially, every 5 transects). Therefore, the number of transects in the area was reduced to 15 to 22 per barrier. An example of the evolution of barrier, dune and marsh for Barreta is given in Figure 14. These calculations were performed for all barriers and environments.
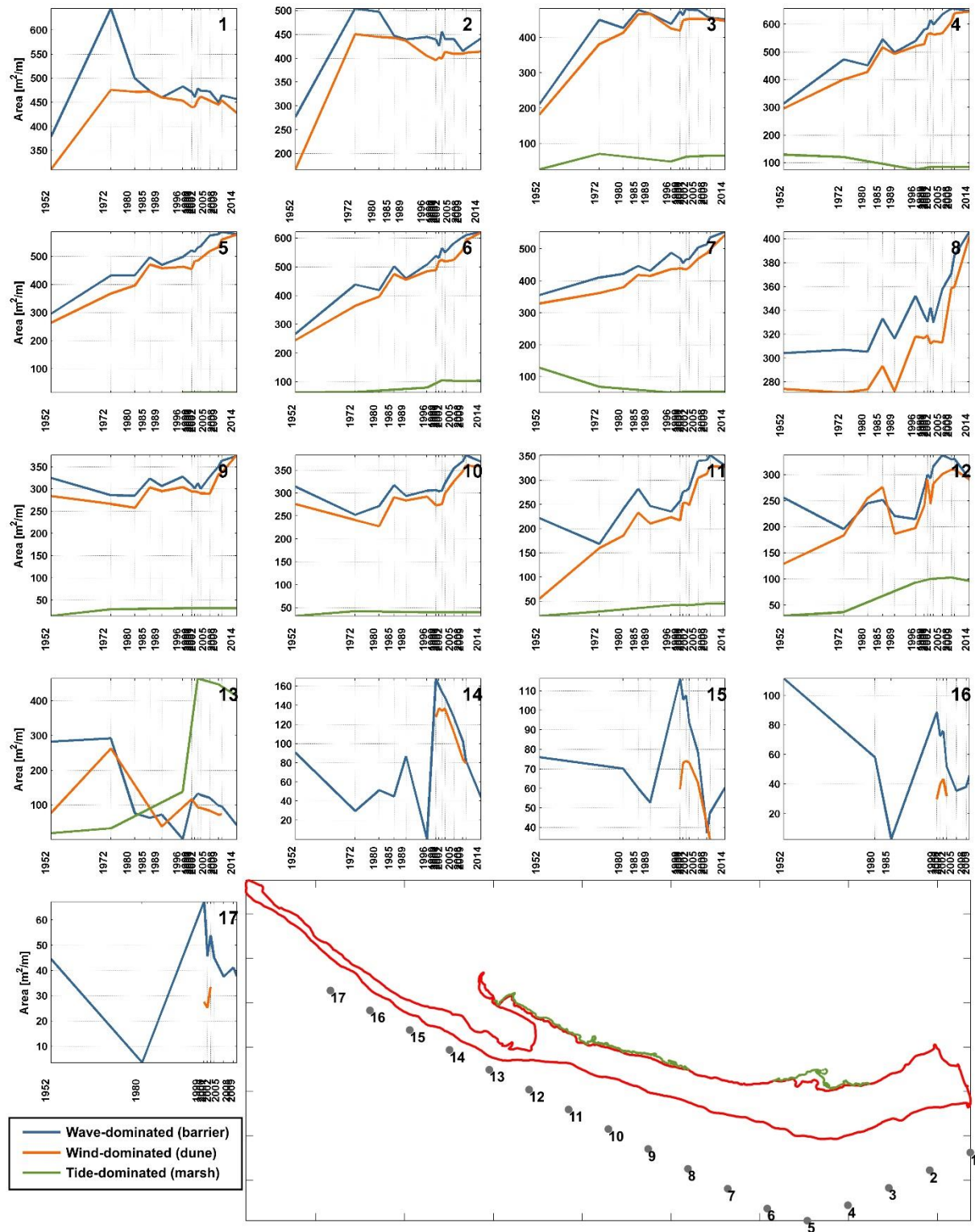
Figure 14: Evolution of widths for all environmental units (wave-, wind- and tide-dominated), averaged over 500 m along the baseline. The numbering is from E to W and corresponds to the locations shown in the map below.

18

It is evident from Figure 14 that some transects have similar evolution. To extract more generalised results that refer to larger barrier parts, the similarity of adjacent sections was estimated calculating the correlation coefficient between neighbouring transects (e.g. transects 1 and 2, 2 and 3, etc.). High correlation coefficients (above 0.7), along with visual comparison of the evolution in each pair, determined whether two successive positions belong to the same group, or not.

An example for the correlation coefficients calculated for Barreta is shown in Figure 15. The values show high similarity between transects 11 and 12, but very low one for 12 and 13. Therefore, transects 11 and 12 should be grouped, whereas 12 and 13 belong to different groups.
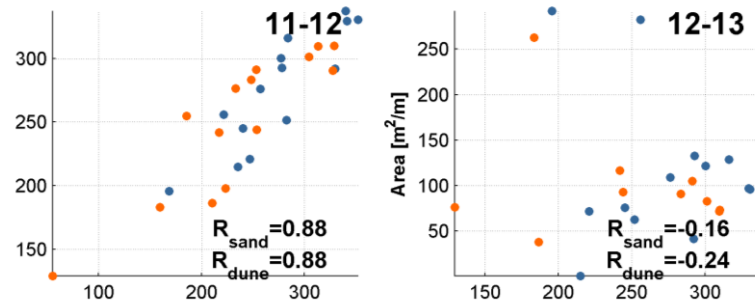
Figure 15: Example from the calculation of correlation coefficients for neighbouring transects (only the pairs 11-12 and 12-13 are shown; see Figure 14 for location) as grouping criteria.

4.2.2 Results

The results for temporal evolution of barrier width, its position (distance from a lagoon-side baseline or from mainland for C-C) are presented further down, moving on from Ancão towards C-C (W to E).

Figure 16 shows the barrier (wind and wave dominated) width and position for the Ancão Peninsula, after grouping of sections with similar evolution. The results for the widths of the distinct geomorphological units examined are also presented in Figure 17, in the form of width values (right-hand axis) and as width percentage that belongs in each unit. The latter was defined assuming a maximum total (sum of all units) width value for each group of transects and using this value as a divisor. Thus, the values for each group of transects vary within 0 and 100%, showing, in this way, the temporal changes in-between units, as well as the presence/absence of environments. It is noted that the presentation of wave-dominated barrier widths in Figure 17 is different from the one in Figure 16. In the latter the value corresponds to the entire barrier width (distance from backbarrier to ocean-side debris line), while in the former the value is the backshore width (distance from foredune to ocean-side debris line, ca. MHHWL to MHWL). Thus, the summation of wind and wave dominated widths in Figure 17 equals the wave-dominated widths shown in Figure 16 (total barrier width).

The values show that the western-central part (1-12; 0 to 6 km downdrift) appears stable from 1952 to 1986 and presents reducing widths since 1986. The marsh widths show stability, while minimum dune widths were noted in 1999. The distance from the baseline (Figure 16) is reducing throughout the period due to the erosive tendencies in the area. The central-eastern part (13-17; 6 to 8.5 km downdrift) show similar evolution in terms of dune and backshore widths, with limited marsh growth and destruction between 1952 and 2001. The eastmost part of the peninsula (18-20; 8.5 to 10 km downdrift) is highly variable, with low widths and an absence of barrier in the area between 1996 and 2005 due to the relocation of the Ancão in 1997 (Vila-Concejo et al., 2002), which is most likely also related to the marsh destruction in transects 13-17 after 1996. The high variability in barrier width in the area is due to inlet dynamics, while there is a consistent tendency for seaward migration.

Figure 16: Evolution of width (top panel) and distance from baseline (bottom panel) for the grouped transects of Ancão Peninsula. The numbering of the grouped transects corresponds to the locations shown on the map.

Figure 17: Evolution width as percentage (with reference to the right axis) and as meters (with reference to the left axis) for the grouped transects of Ancão Peninsula. The wave-dominated barrier here corresponds to backshore and the numbering of the grouped transects corresponds to the locations shown on the map.

The evolution of barrier widths and position of Barreta are given in Figure 18 and in Figure 19 (as percent and absolute widths, with the wave-dominated barrier to correspond to backshore). The area adjacent to the F-O Inlet (1-4; 0 to 2 km westwards), that essentially is the part of the barrier belonging to the east flank of Ria Formosa, presents intense growth until 1972 and, since then, shows only small-scale variability. The central part (5-12; 2 to 6 km east from the jetty) is growing throughout the study period and, at the same time, expanding seawards, with average rates of 2.5 m/yr and 3.4 m/yr for the wave and wind dominated parts of the barrier, respectively. Dune growth in the both the east and the central parts is constant and the marsh appears stable after 1972. In the area near the Ancão Inlet (13-16; 6 to 8 km west from the jetty), there is a tendency for barrier reduction (wind and wave dominated) and for seaward migration. The absence of barrier from 1989 to 1999 is due to the natural eastward migration of the Ancão inlet, while the reestablishment of the units after 1999 is due to its artificial relocation.

Figure 18: Evolution of width (top panel) and distance from baseline (bottom panel) for the grouped transects of Barreta Island. The numbering of the grouped transects corresponds to the locations shown on the map.

Figure 19: Evolution width as percentage (with reference to the right axis) and as meters (with reference to the left axis) for the grouped transects of Barreta Island. The wave-dominated barrier here corresponds to backshore and the numbering of the grouped transects corresponds to the locations shown on the map.

The analysis of environmental units' widths and relative position is given in Figure 20 and Figure 21. The area directly downdrift from F-O Inlet (1-7; 0 to 3.5 km to the east of F-O) presents a constant reduction in barrier (backshore) and dune widths and, as a result, a landward shift of the related centroids, directly related to sediment starvation from the jetties. The marshes in the area are stable and appear fully developed since the 1970s. In the central part (8-9; 3.5 to 4.5 km) there is fast barrier and dune growth until 1972 and, from then on, the variability increases, mainly due to hydrodynamic forcing conditions. The area starts to develop marshes after 1985 that appear stabilised since 2000. The eastern, newer part of the island (10-15; 4.5 to 7.5 km eastwards), was formed after 1972 and obtained maximum barrier width by the 1980s. Marsh development appears in 1996 and the growth appears stabilised by 2005.

Figure 20: Evolution of width (top panel) and distance from baseline (bottom panel) for the grouped transects of Culatra Island. The numbering of the grouped transects corresponds to the locations shown on the map.

Figure 21: Evolution width as percentage (with reference to the right axis) and as meters (with reference to the left axis) for the grouped transects of Culatra Island. The wave-dominated barrier here corresponds to backshore and the numbering of the grouped transects corresponds to the locations shown on the map.

23

The related results of short-term changes in the averaged sections of Armona are given in Figure 22 and Figure 23. The west part (1-4; 0 to 2 km east from the Armona Inlet) shows continuous barrier and dune growth (and corresponding seaward movement of the centroid), as result of the changes in the tidal prism of the Armona Inlet, initiated by the stabilisation of F-O. The growth is near-linear for both environments, with average rates of 3.6 m/yr. The marshes in the area appear stabilised, especially after the 1980s. In the west-central part (5-7; 2 to 3.5 km downdrift) the overall tendency is one of growth, but with a high inter-annual variability, probably due to storm impacts; the area shows fully developed marshes throughout the study period. The central part (8-12; 3.5 to 6 km downdrift) shows dune growth, high storm variability in the backshore area and marsh stability after 1985. In the central-east part (13-16; 6 to 8 km downdrift), which a low-width part of the barrier, highly impacted by the migration and dynamics of the Fuzeta Inlet, a general erosion tendency is identified, for both wind and wave dominated units. Strong variability is noted in the marsh development, with high rates up to the late 1980s and marsh destruction from 1990 to 2009 that are related with the inlet dynamics. In the eastern part (17-19; 8 to 9.5 km downdrift), the barrier is present from 1972 to 2009, with a seaward tendency, relatively stable dune widths and more variable backshore widths.
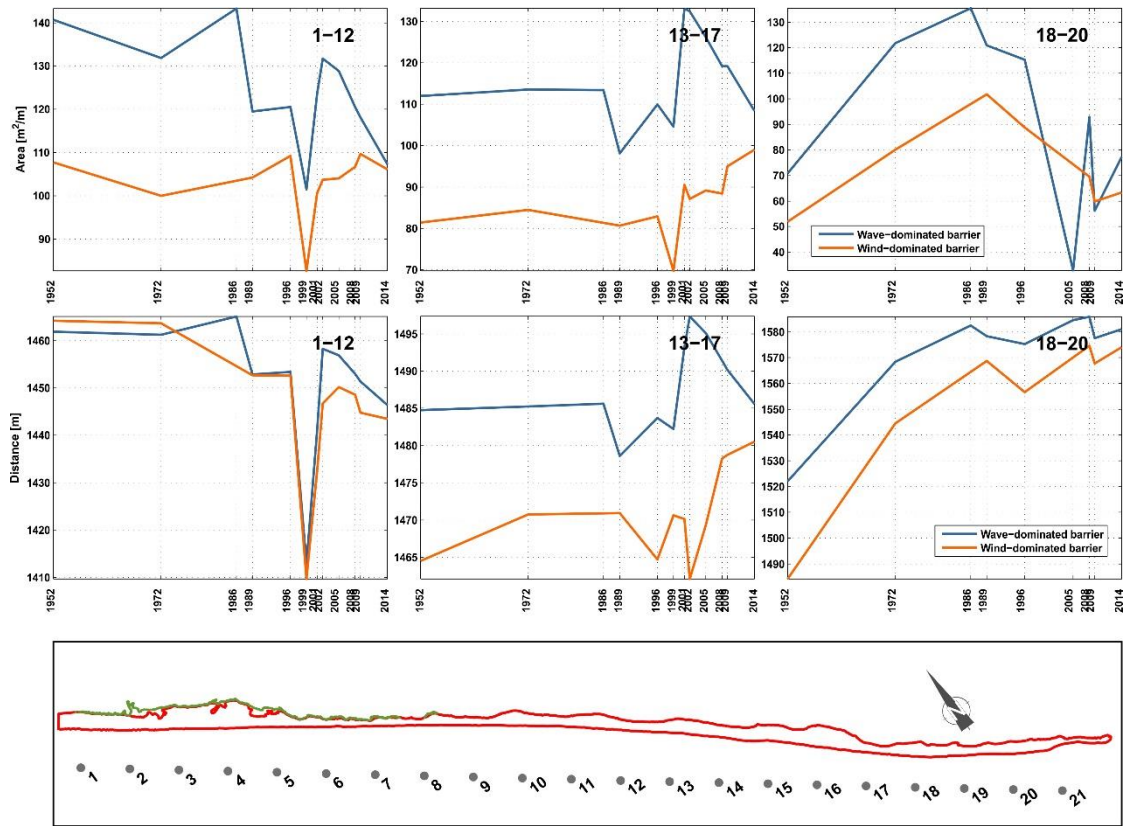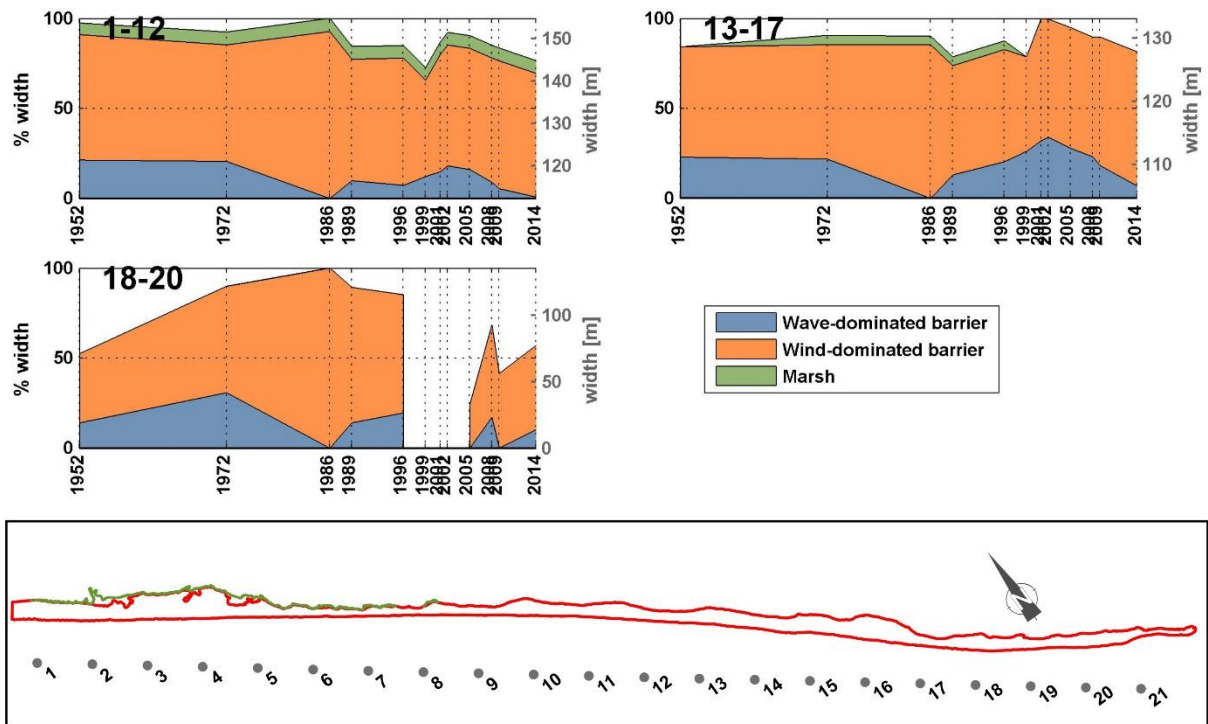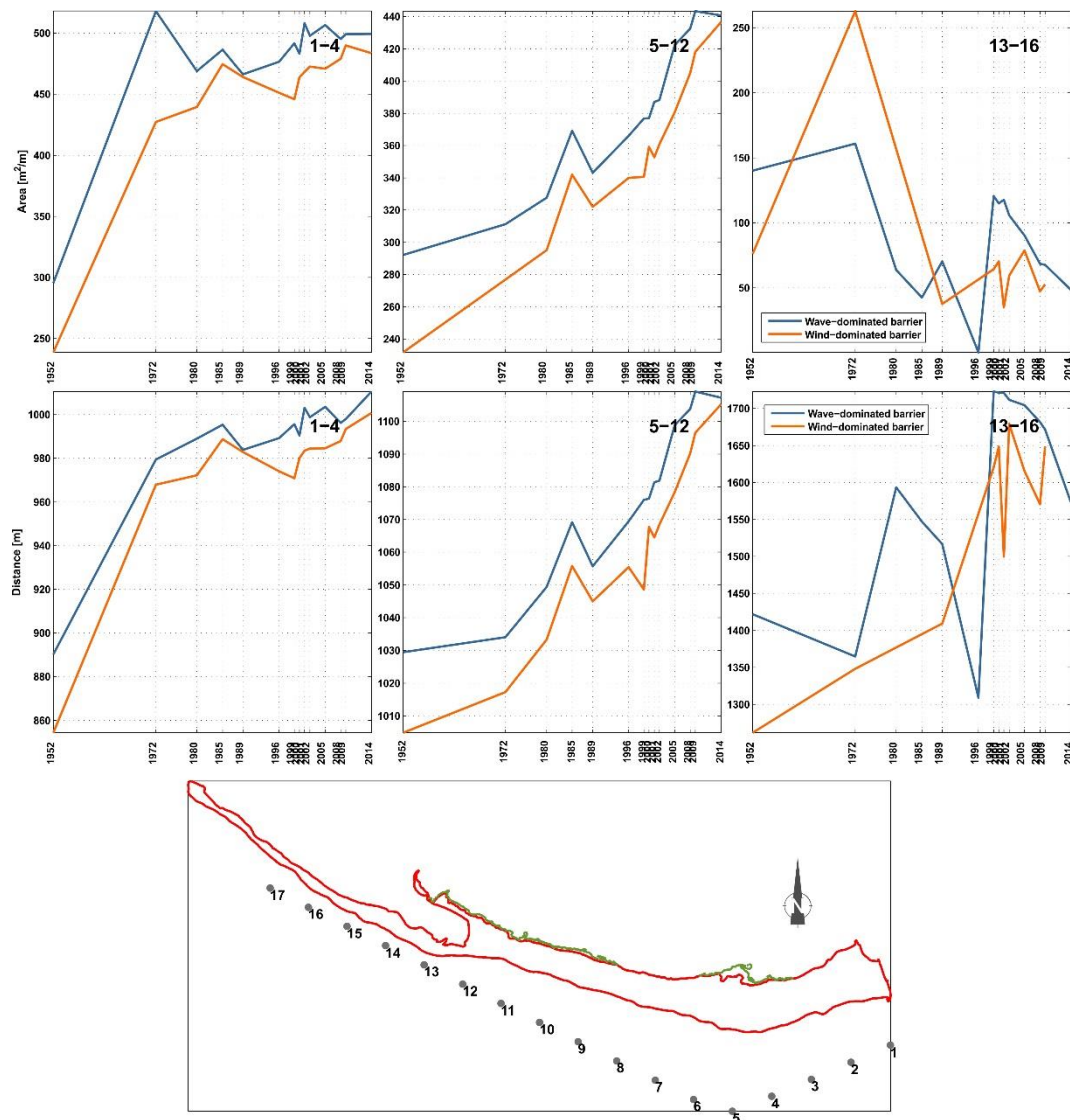
Figure 22: Evolution of width (top panel) and distance from baseline (bottom panel) for the grouped transects of Armona Island. The numbering of the grouped transects corresponds to the locations shown on the map.
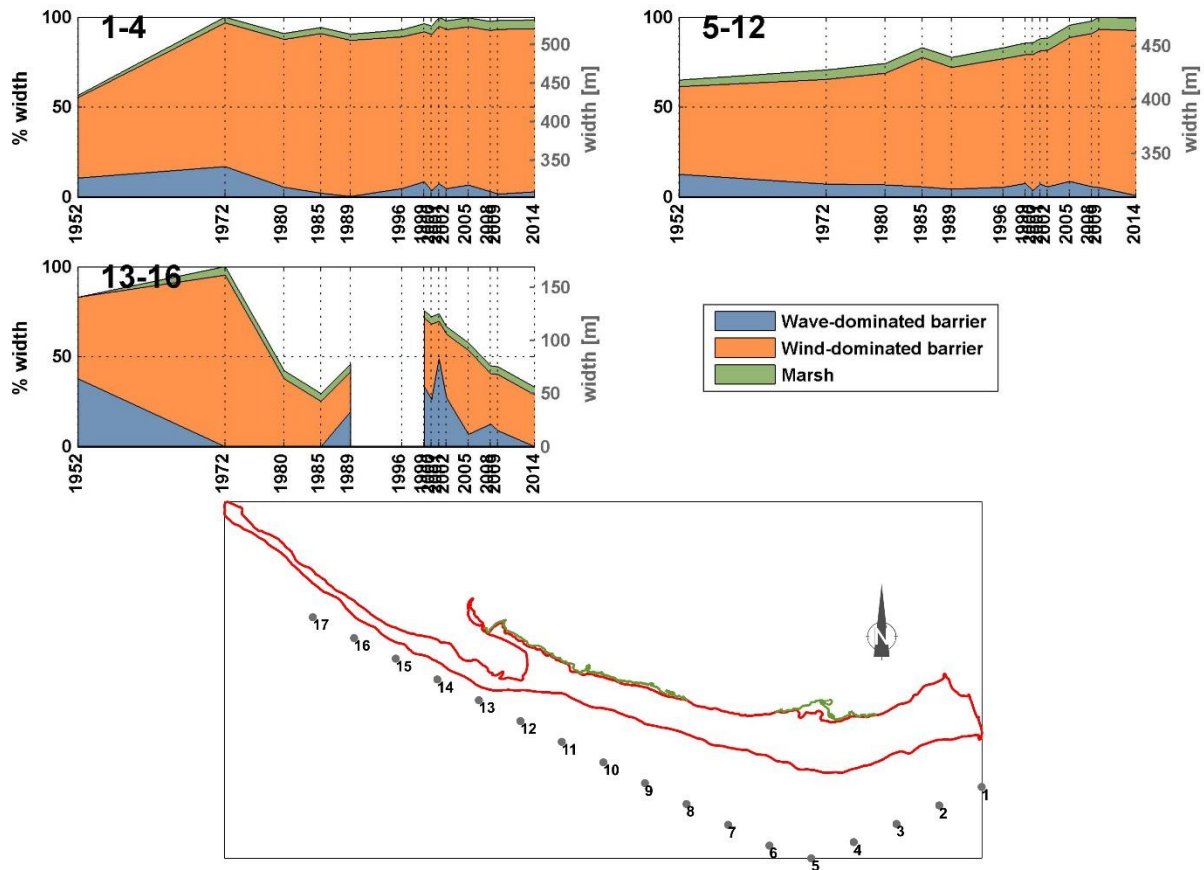
Figure 23: Evolution width as percentage (with reference to the right axis) and as meters (with reference to the left axis) for the grouped transects of Armona Island. The wave-dominated barrier here corresponds to backshore and the numbering of the grouped transects corresponds to the locations shown on the map.

The results for Tavira are presented in Figure 24 and Figure 25, with the transect numbering to increase from east to west. The west part (1-6; 0 to 3 km updrift from the Tavira jetty) shows constant barrier and dune growth due to the sediment accumulation against the jetty. No marsh is present in the area due to the proximity of the channel to the backbarrier. In the central-eastern part (7-14; 3 to 7 km updrift from the jetty), limited coastal retreat is noted. However, the barrier has maintained substantial average widths (over 1000 m) throughout the study period with low backshore widths and widespread dune fields. The marsh platform is also wide and very stable, especially after the 1980s. The central-western part of the island (15-19; 7 to 9.5 km updrift from the jetty), with lower barrier widths, also shows dominant erosive tendencies, combined with stable and broad marshes in the lagoon side. In the west part (20-22; 9.5 to 11 km updrift from the jetty), near the Fuzeta inlet, the barrier becomes significantly narrower, and the temporal variability higher. Generally, a tendency for coastal and dune retreat is noted up to 1989, followed by a period of coastal progradation and dune growth. The backbarrier environment and marsh is stable throughout the period.
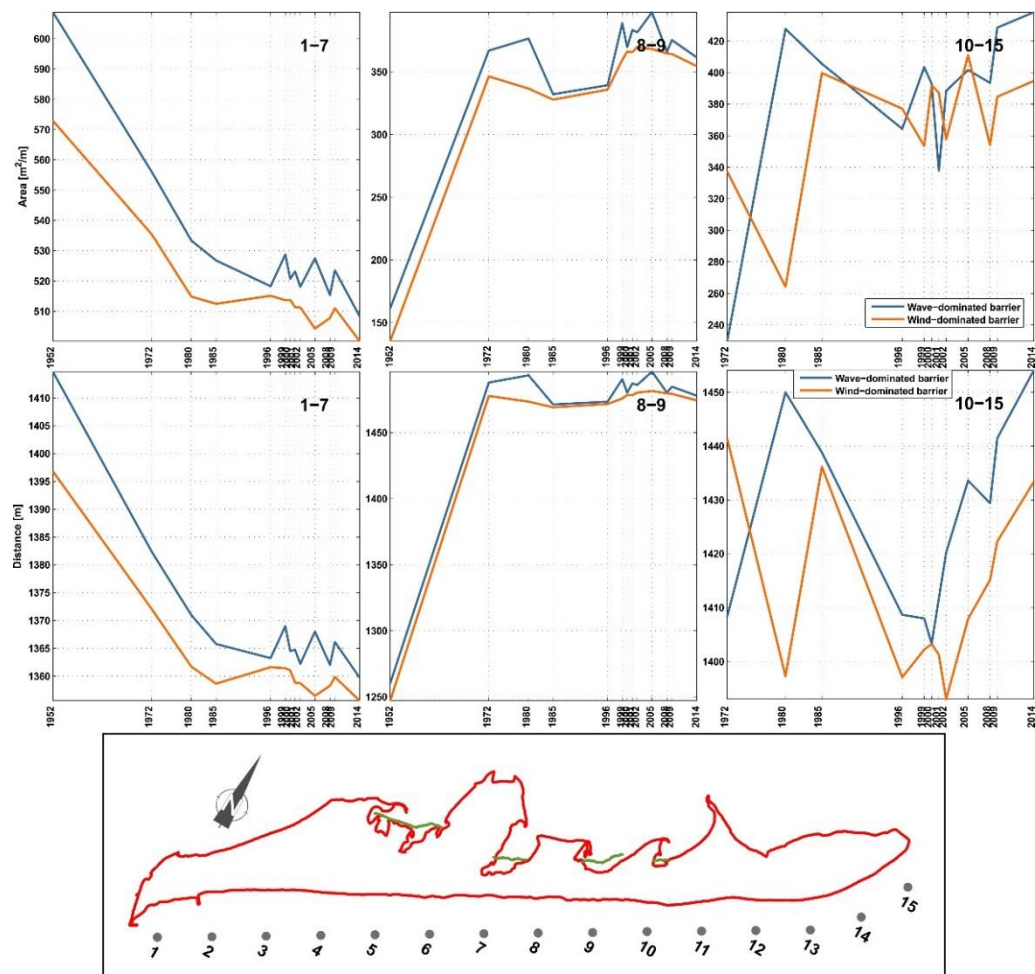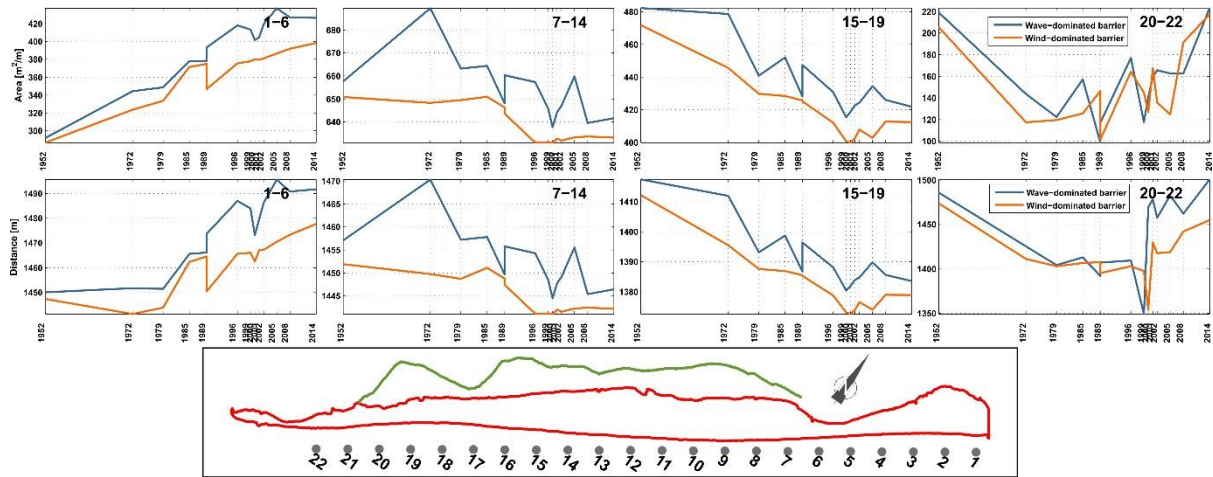
Figure 24: Evolution of width (top panel) and distance from baseline (bottom panel) for the grouped transects of Tavira Island. The numbering of the grouped transects corresponds to the locations shown on the map.
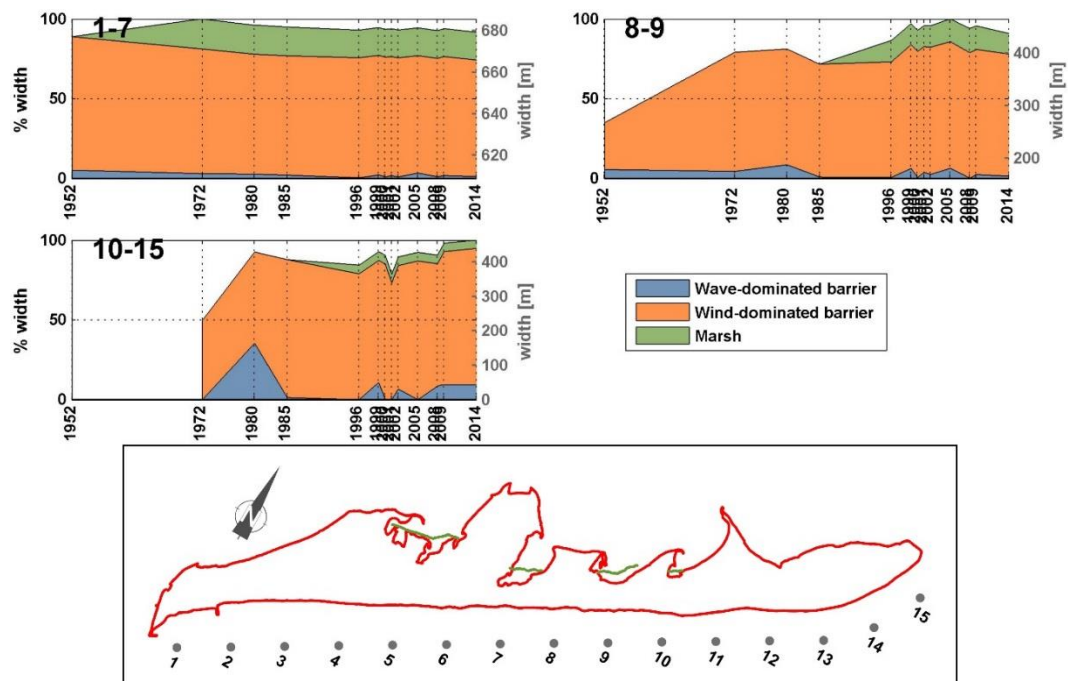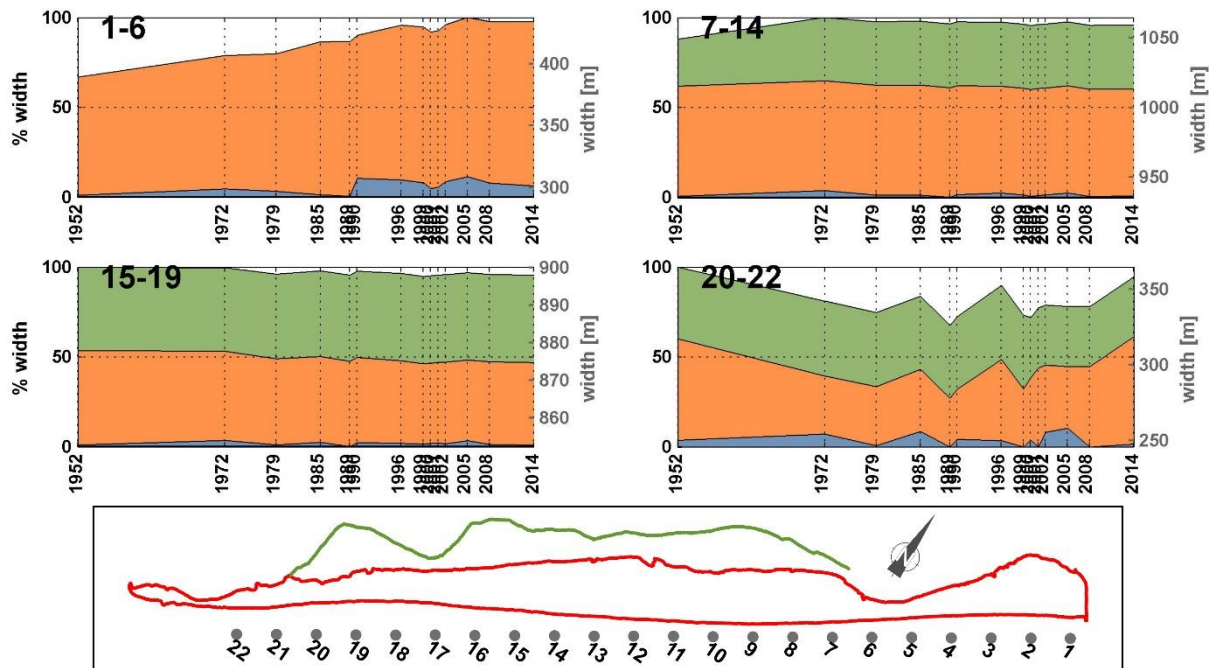

Figure 25: Evolution width as percentage (with reference to the right axis) and as meters (with reference to the left axis) for the grouped transects of Tavira Island. The wave-dominated barrier here corresponds to backshore and the numbering of the grouped transects corresponds to the locations shown on the map.

For C-C the short-term evolution is given in Figure 26 and Figure 27, for the grouped transects from west to east, where the different phases of evolution (before and after 1986) are clearly identified. The west part (1-3; 0 to 1.5 km from the E Tavira jetty) appears after 1972 and corresponds to the west part of Cabanas, showing increasing tendency for growth and seaward expansion until 1986 and with limited erosive trends and reduction of the distance from mainland, thereafter. Marshes start developing in the area after 1985, with high variability in marsh widths, most likely related to overwash events. The central part (4-12; 2 to 6 km from the jetty) shows clear transgressive behaviour until 1986, with dune and shore erosion and related reduction in the widths of all analysed geomorphological units. Following 1986 the widths of all three units is increasing until the end of the study period, while the mean barrier position is migrating seawards (mainly due to seaward expansion). Therefore, following 1986 the C-C system appears to enter a period of recovery after a

26

period of constant rollover, which is also accompanied by significant marsh growth. The east part (13-18; 6 to 9 km from the jetty) shows a predominant erosion tendency in all geomorphological units. It is noted that after 1996 this part has been highly affected by the eastward migration of the Lacém Inlet, as well as by the breaching event of 1995-96 in Cacela (Figure 11), which caused high losses in barrier and dune widths. Thereafter, there is limited barrier growth, but without significant dune recovery.
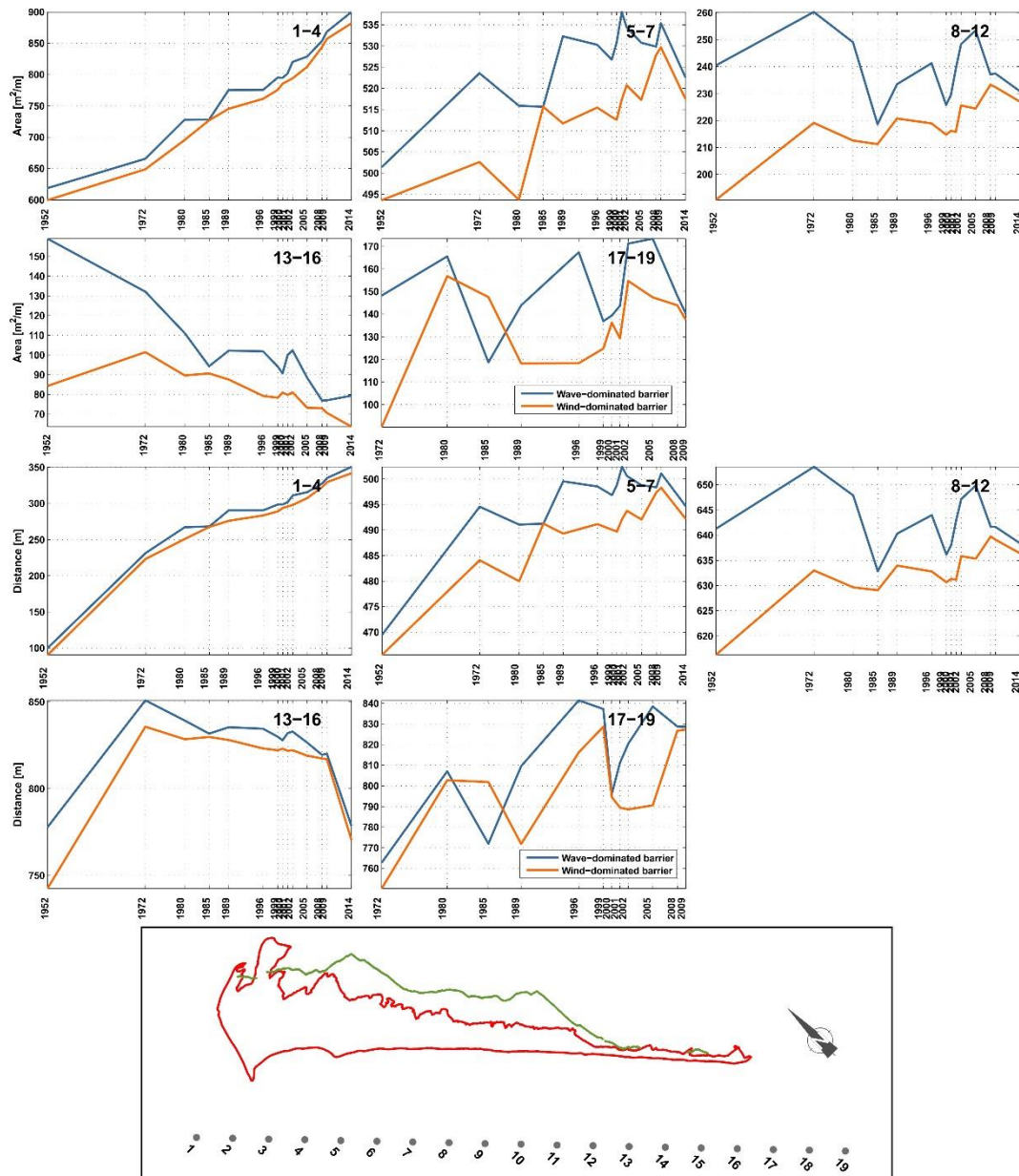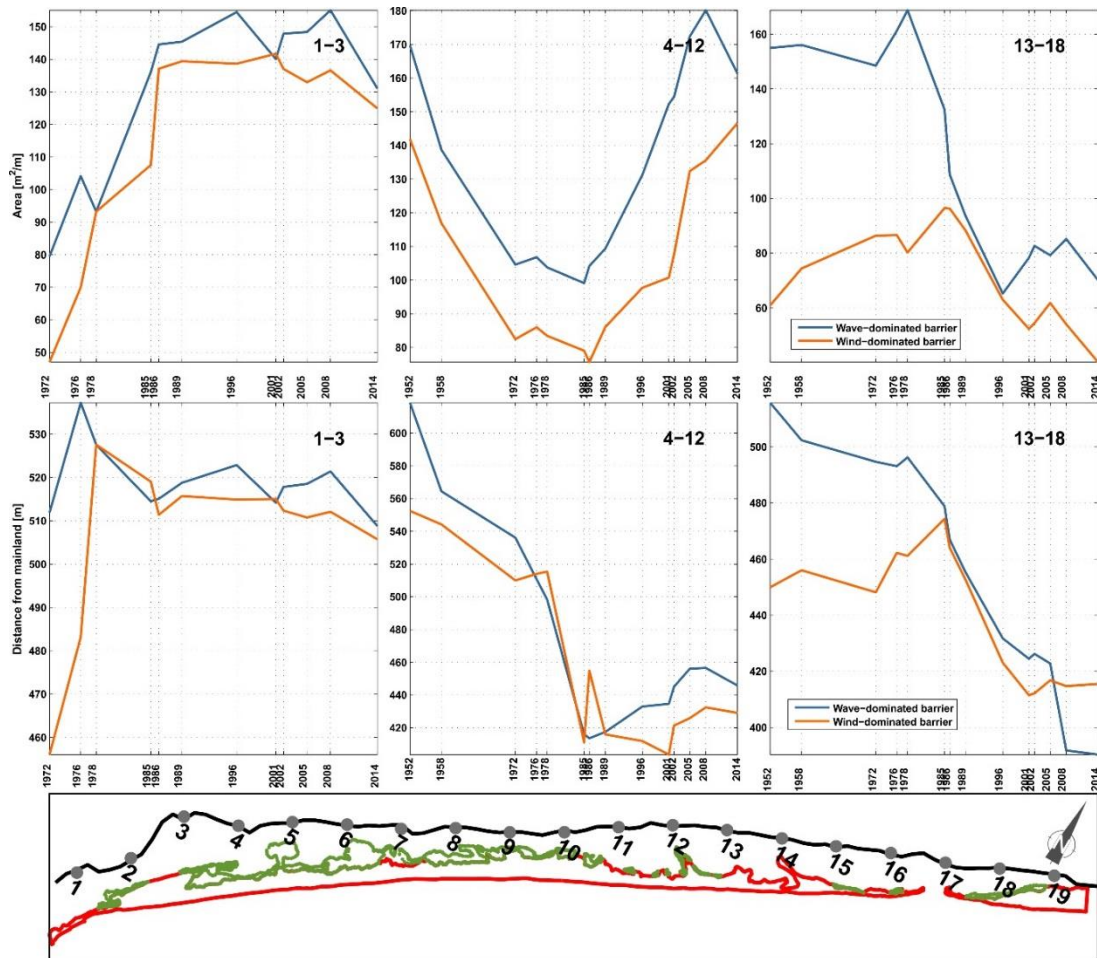

Figure 26: Evolution of width (top panel) and distance from baseline (bottom panel) for the grouped transects of Cabanas-Cacela. The numbering of the grouped transects corresponds to the locations shown on the map.
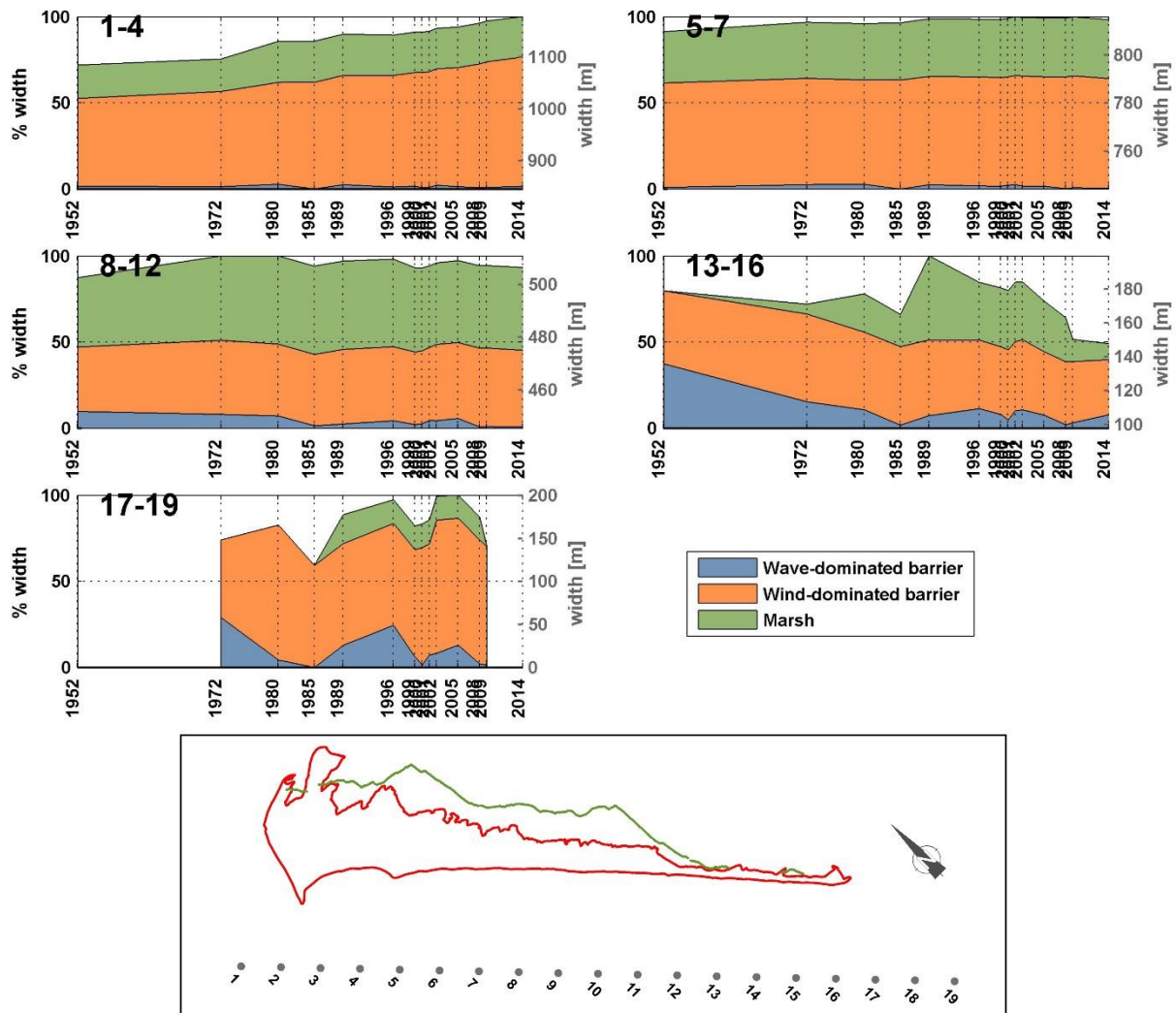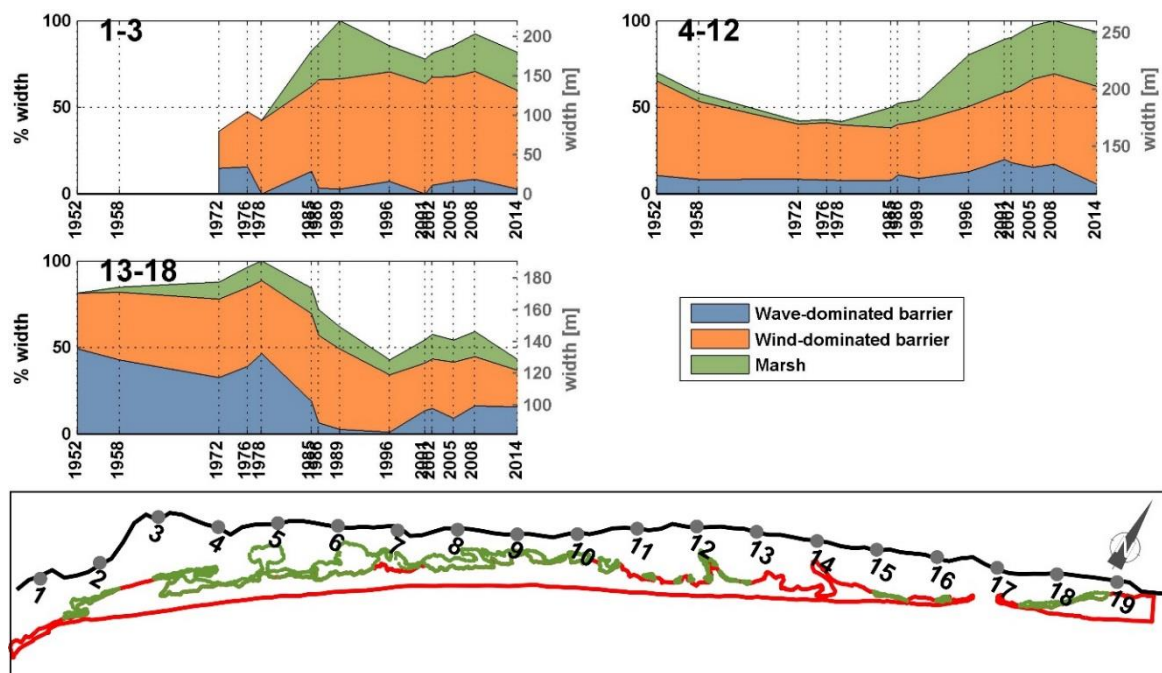
Figure 27: Evolution width as percentage (with reference to the right axis) and as meters (with reference to the left axis) for the grouped transects of Cabanas-Cacela. The wave-dominated barrier here corresponds to backshore and the numbering of the grouped transects corresponds to the locations shown on the map.

5. LONG-TERM EVOLUTION OF GEOMORPHOLOGICAL UNITS

5.1 Morphological Evolution Trends

5.1.1 Barrier – Wave dominated

To analyse the evolution of the barriers in relation with the wave activity and human interventions, the total area of the barriers was calculated and is presented in Figure 28 for the west flank and in Figure 29 for the east flank. The barrier area is plotted as change relative to the first available recording (1952), along with the average annual significant storm wave height and total annual storm duration. Significant interventions in the area are also noted in the timeline, along with breaching events in each flank.

In the west flank (Figure 28), it can be noted that the evolution of Ancão and Barreta is highly interlinked, with the growth of one barrier to be largely followed by a reduction of the other. Ancão presents accretion in the period of 1952 to 1972, related with the eastward migration of the Inlet. In the same period, Barreta is growing southwards due to the stabilization of the downdrift F-O Inlet. The storms of 1973 caused the breaching of a second inlet in the peninsula (Vila-Concejo et al., 2002), initiating losses for Ancão and corresponding gains for Barreta. From 1976, the inlet started an eastward migration cycle, reaching its eastmost position in 1996, which is reflected in the slow growth of Ancão and the reduction of Barreta barrier areas following 1985. The reduction in Ancão between 1972 and 1985 is attributed to the construction of the Vilamoura jetties, around 10 km west (updrift) from the Peninsula, that reduced the longshore drift reaching Ancão (Ferreira, Garcia, Matias, Taborda, & Dias, 2006). In June 1997, extensive coastal management work was performed in Ria Formosa, including the relocation of Ancão Inlet (Vila-Concejo et al., 2002). This is reflected in the evolution of Ancão and Barreta, with significant drop to the former and related increase to the latter that lasted up to 2002, where the inlet reached its westernmost point. Subsequently, a new eastward migration cycle started, coincident with beach nourishment projects in Ancão ($2.65 \cdot 10^6$ m³ distributed in Ancão, Armona, Tavira and Cabanas) (Dias, Ferreira, Matias, Vila-Concejo, & Sá-Pires, 2003) and in the updrift coastal zone (1998, 2004 & 2010) (Oliveira, Catalão, Ferreira, & Alveirinho Dias, 2008) that increased sediment availability in the area and halted coastal retreat in Ancão. From 2002 onwards, Ancão and Barreta showed only small-scale changes (within ±5%). Taking into account that longshore sediment transport is directed eastwards and assuming that the sediment bypassing the F-O jetties is low, the summation of the area of the two barriers (dashed blue line in Figure 28) can reveal the direct impacts of the F-O stabilisation to the sediment balance of the western flank. The curve shows that the accumulation of sand initiated by the F-O jetties was intense up to 1985, reaching 15% in 33 years. From 1985 the values vary with the total increase in the period, compared to 1952 to range within +5 and +15% with an overall, average increase of +10%. At present, the width of Barreta has reached the width of the jetty (grey-filled curve in Figure 6) and accumulation is occurring as submerged sand banks in front of the island (Pacheco, Vila-Concejo, Ferreira, & Dias, 2008).
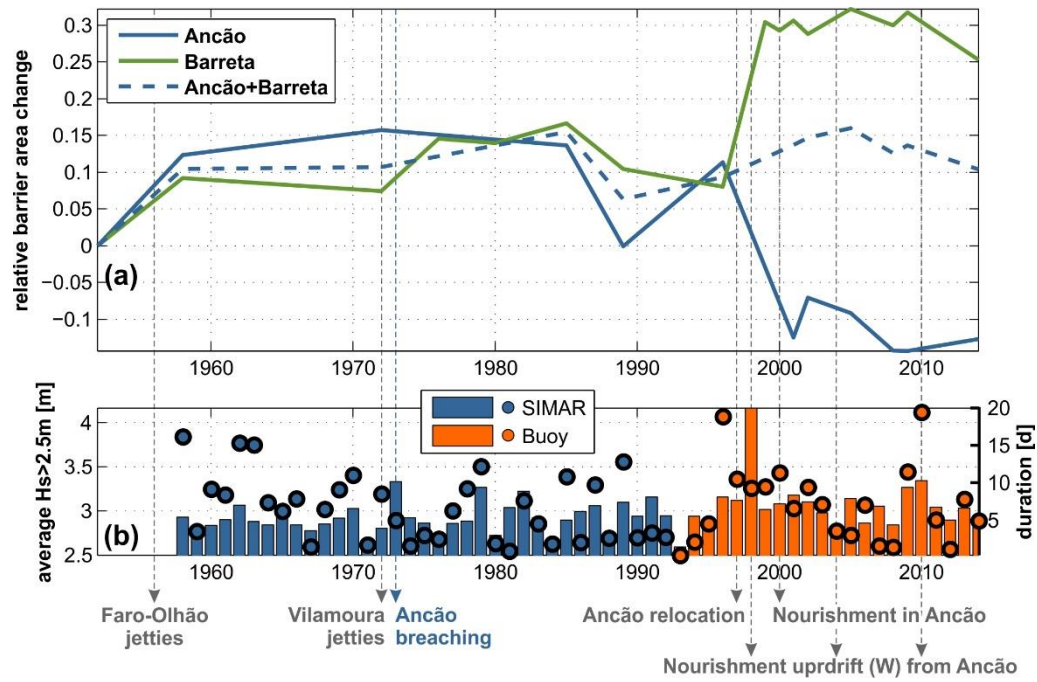
Figure 28: Evolution of total barrier area, relative to 1952 (a), and storm wave data (b) for the west flank. Wave data include average significant storm wave heights (bars, with reference to the left axis) and total annual storm duration (scatter-points, with reference to the right axis) at the location of the Faro buoy; data after 1993 are buoy records and older ones are SIMAR hindcasting data (Spanish State Port Authority). Human interventions (grey and black arrows: W from the area) and Inlet breaching events (arrows coloured as the related barrier) are noted.

In the eastern flank (Figure 29), Culatra and Armona present a growing tendency almost throughout the study period. This growth is also attributed to the stabilisation of F-O that, as mentioned previously, induced the reduction of the tidal prism of the in-between Armona Inlet. The growth of Armona is also affected by the eastward migration of the Fuzeta Inlet, migration that also impacts the downdrift barrier of Tavira. To elucidate the evolution of the barriers and the 'net' contribution of the stabilisation works (F-O and Tavira jetties), Armona was split in two parts, W and E (see Figure 1 for location), which were added to each neighbouring barrier, assimilating, in this manner, the short-term, strong morphological changes due to the Fuzeta Inlet movement. Thus, the joined barrier evolution of Culatra and west Armona (Culatra+Armona W in Figure 29a) and of east Armona and Tavira (Armona E+Tavira in Figure 29a) can be studied. Given that the margins of these two groups correspond to stabilised inlets (F-O to the W and Tavira to the E), the ocean-side longshore gains and losses of the total area can be omitted. As shown by the evolution of Culatra and Armona W, the area is growing continuously throughout the study period, with a linear trend of $2.6 \cdot 10^4$ m^2/yr (R^2=0.97), reaching an increase of 38% in 2014, compared to 1952. Small-scale shifts to the relative change of the accumulated sand area are attributed to storm events (e.g. trend reduction between 1980-85, due to the intense wave activity of 1983). The evolution of Tavira shows reduction in total area, however, after the addition of Armona E the curve shows low variability, within ±5% (orange solid vs. dashed lines in Figure 29a); it, thus, becomes evident that the reducing trend in the area of Tavira is due to the migration of Fuzeta and not to storm impacts. The extension of the Tavira jetties in 1985 seems to invoke limited sediment accumulation that lasts up to 1997, after which, slightly decreasing trends are observed, most likely related to the highly energetic storms and to long-lasting events (Figure 29b). The beach nourishment of 1999-2000 in Tavira and Armona (Dias et al., 2003) caused an increase in barrier area up to 2005, after which the area slightly dropped due to storm conditions. The C-C barriers present relative stability in total area for the period of 1952 to 2002, with the values to fluctuate within

±10%, mainly due to storms and overwash events. More specifically, for the period during which the subsystem was transgressing (1952 to 1986), the area losses were lower than 20%; initially the barrier area was reducing, with peak losses in 1976 that coincided with an inlet breach in Cabanas, after which the subsystem managed to regain the area it occupied in 1958, within 10 years (1986). From then on the roll-over of the barriers ceased and the system begun to advance seawards. At the same time, the Tavira jetties were also extended in 1985, which appears to have induced a new cycle of barrier loss, that lasted up to the 1990s. From then on, the system grew continuously up to 2008, with peak growth of 12%, relative to 1952. This growth is most likely assisted, or even initiated, by the human interventions in the area, in the form of dune and beach nourishments. From 2008 onwards, small losses, probably caused by storms, reduced the total barrier area at the levels of the initial values of 1952.
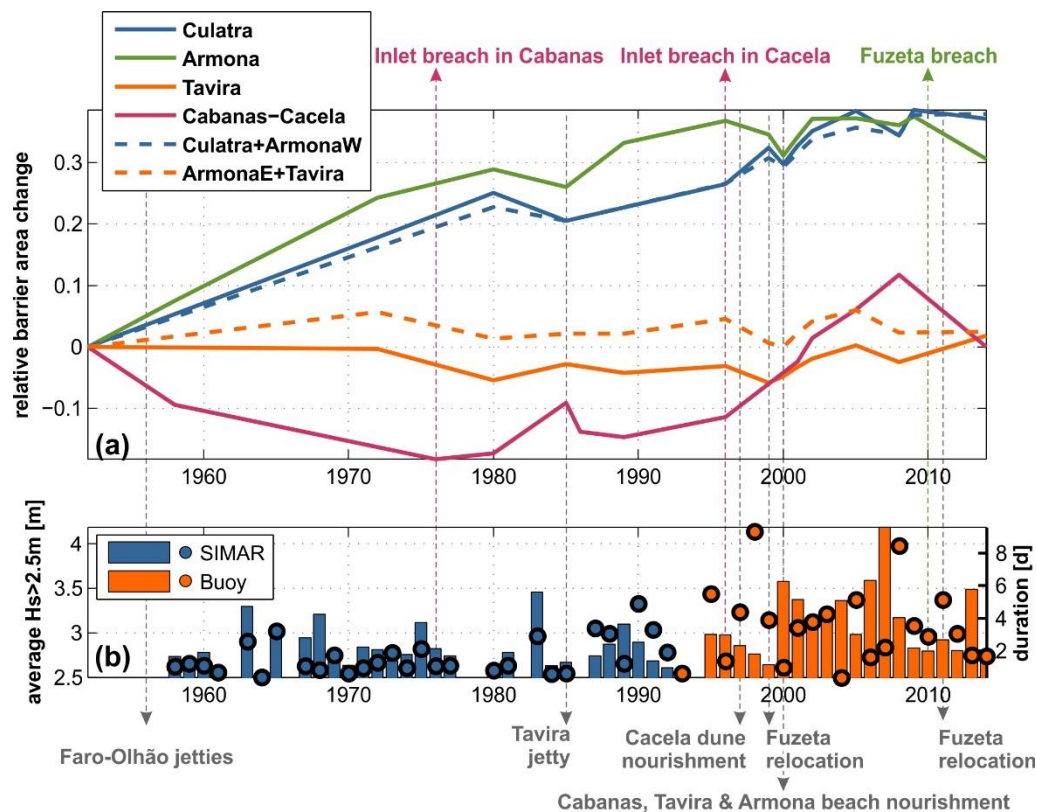
Figure 29: Evolution of total barrier area, relative to 1952 (a), and storm wave data (b) for the east flank. Wave data include average significant storm wave heights (bars, with reference to the left axis) and total annual storm duration (scatter-points, with reference to the right axis) at the location of the Faro buoy; data after 1993 are buoy records and older ones are SIMAR hindcasting data (Spanish State Port Authority). Human interventions (grey and black arrows: W from the area) and Inlet breaching events (arrows coloured as the related barrier) are noted.

The evolution of barrier area in Ria Formosa as a whole is presented in Figure 30, in terms of values and as percentage change relative to the start of the study period. It can be noted that there has been net barrier area gains during the study period, with values that reach 20%. This shows that, overall, the barrier system was effective in trapping and incorporating sediment, either from the long-shore sediment transport or from shoals in the lagoon, as well as balancing the erosive impact of storms and human pressures. It can be noted that the trend of barrier area growth is significantly lower after 2000, which could mean that the barrier system is reaching some sort of peak growth.
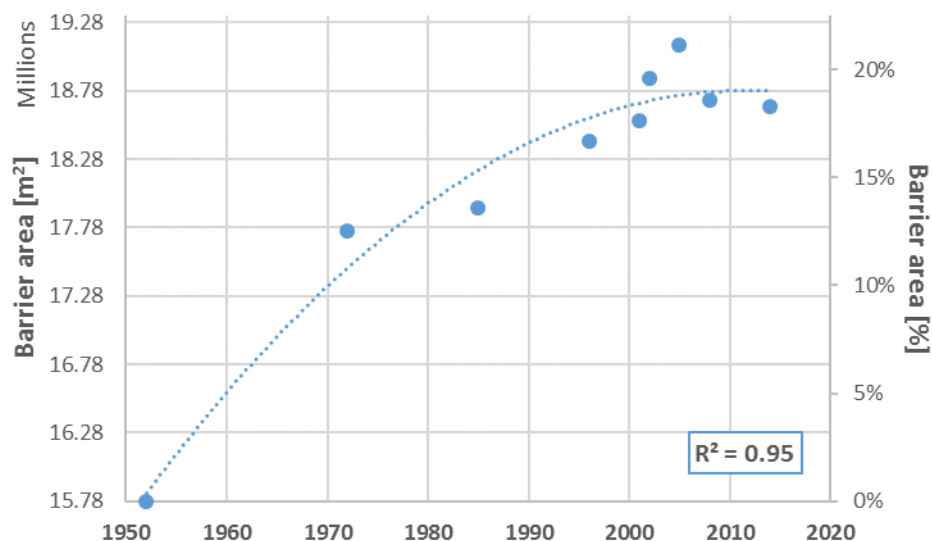
Figure 30: Evolution barrier area for all the barriers in Ria Formosa; the left vertical axis presents the values in m² and the right vertical axis as a percentage; the fitted trend line is a 2nd order polynomial.

5.1.2 Marshes – Tide dominated

The total marsh area, perched to the backbarrier of each barrier, was defined using the boundaries of backbarrier and marsh edge lines to delimit the respective polygons. The temporal evolution of these values is presented and discussed further down.

Regarding the marshes in the barriers of the west flank (Ancão and Barreta), their temporal evolution is given in Figure 31. For Ancão, there is limited temporal variability in marsh area, with the values fluctuating between 5.6 and $7.5 \cdot 10^4$ m². After 2000 the values are stabilised to around $7 \cdot 10^4$ m². These marshes are located mainly in the western end of the peninsula and appear stable and mature. For Barreta, an increase of about 700 m²/yr until 2001 is noted, rate that drops to 270 m²/yr from 2001 onwards.
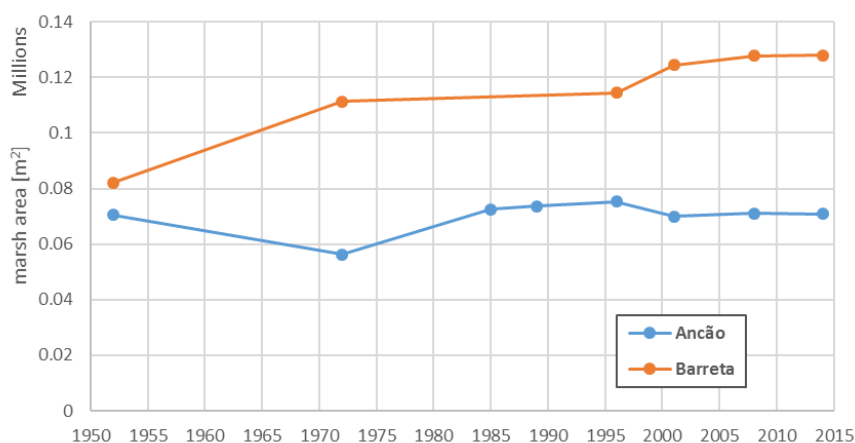
Figure 31: Evolution of marsh area in Ancão and Barreta; the values are in 10^3 m².

For Culatra (Figure 32), the marshes show an overall growing tendency throughout the study period that for the barrier as a whole shows a linear trend of $2 \cdot 10^3$ m²/yr up to 1996 and reduced rates of around 700 m²/yr thereafter. Examining each embayment separately (the location and naming is explained in Figure 33a), the western, oldest marsh of the barrier grows rapidly ($1.5 \cdot 10^3$ m²/yr) up to

1986 and significantly slower thereafter (120 m^2/yr). The same evolution trend is observed for the marsh in the second (from W to E) embayment, with rates of 660 m^2/yr up to 1986 and 75 m^2/yr thereon, and of the fourth embayment, with rates of 250 m^2/yr up to 1986 and 40 m^2/yr from then on. The evolution pattern of the third embayment is somewhat distinct, with rates of 300 m^2/yr up to 1986 and with quadruplicate rates (1.2·10^3 m^2/yr) thereafter (1986-2008). The last mapping of the marshes in the area (2014) shows a small decrease, that could signify that the marshes in the embayment are passing on to mature conditions. The boost in marsh growth after 1986 in this particular embayment is most likely related with the hydro- and sediment dynamics in the area and their relation to the morphology of the island itself. The spit formation in the lagoon side of Culatra (late 1970s), along with the reduction of the tidal prism in the Armona Inlet and the morphology of the bay (wide mouth, funnel-shaped) are probably responsible for enhanced sediment trapping in this particular bay that enabled the increase of marsh platform heights and faster marsh development (Figure 33b). At the same time, the same spit formation is probably responsible for the cessation in the marsh growth of the fourth bay, due to the shadowing effect it produces to the bay (Figure 33b), thus hindering circulation and sediment influx.
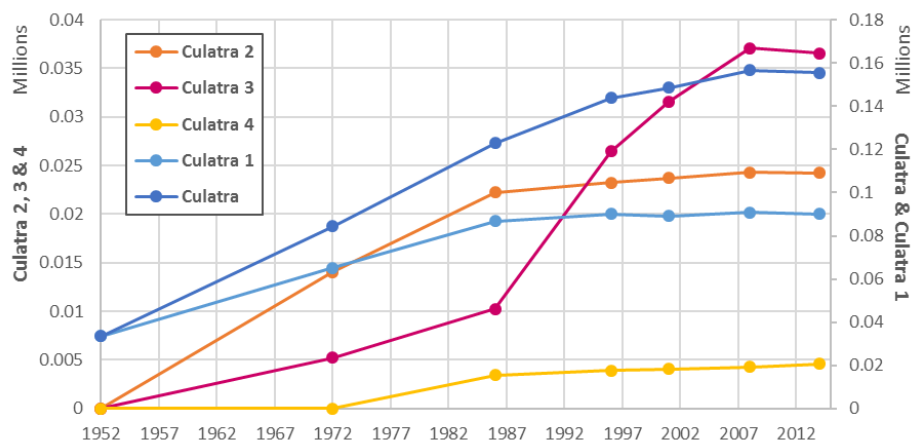
Figure 32: Evolution of marsh area in Culatra (Culatra 1, 2, 3 & 4: marshes of the first, second, third & fourth embayment, from W to E; Culatra: Sumation of all four embayments; Culatra 1 and Culatra refer to the right-hand y-axis); the values are in 10^{3}m^2.
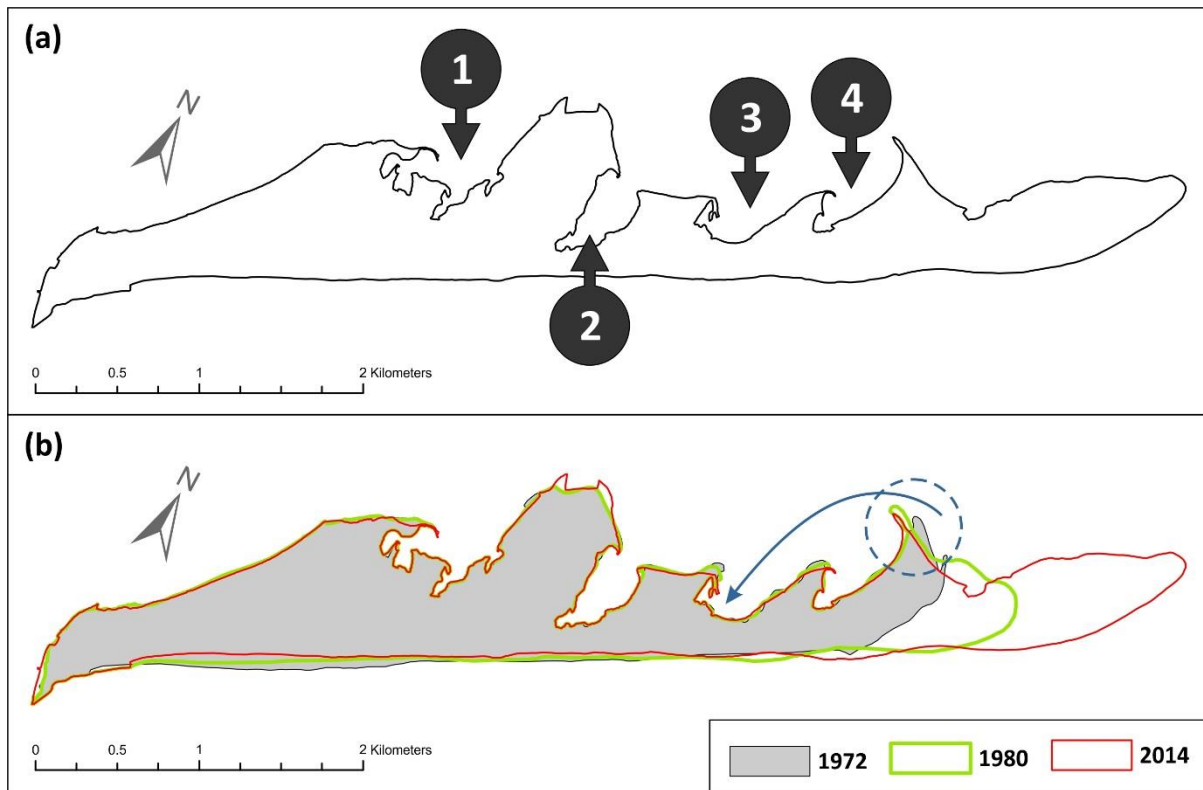
Figure 33: Location of the four embayments of Culatra, noted on the 2014 map (a) and changes in barrier morphology between 1972, 1980 and 2014 that include the formulation of a spit in the lagoon side (noted with dashed blue circle) that increased sediment flow to the 3rd bay (noted with blue arrow) (b).

The evolution of the marshes in Armona and Tavira are shown in Figure 34. It can be noted that for Armona, there is a growth of 10^4 m^2/yr up to early 1990s, but thereafter the trend turns slightly negative, with losses of $1.2 \cdot 10^3$ m^2/yr. These losses are localised at the edges of the channel and are most likely caused by dredging. On the other hand, even though this area loss seems significant, the corresponding maximum loss of marsh corresponds to just 2.3% of the total marsh area of 1989. In Tavira, the marsh has remained at a stable state for the greater part of the study period (since the 1990s). It is noted that Tavira pertains to the most extensive perched marsh in the Ria Formosa system, that appears stable and at a mature conditions (Carrasco, Ferreira, Davidson, Matias, & Dias, 2008).
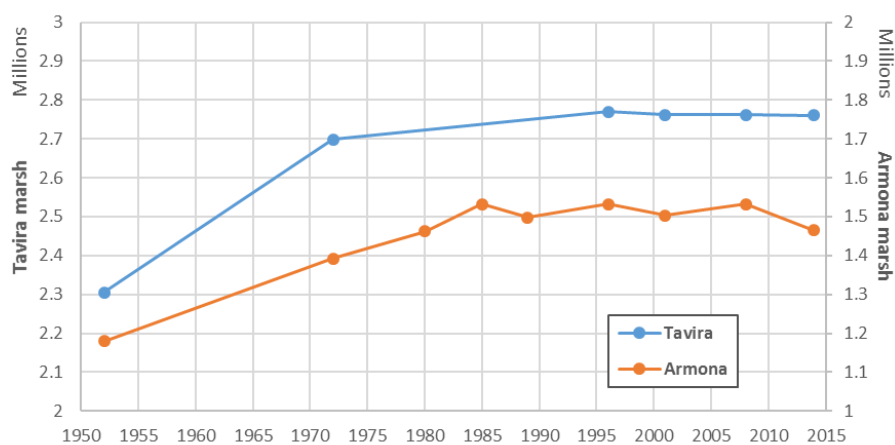
Figure 34: Evolution of marsh area in Armona (with reference to the right-hand y-axis) and in Tavira (with reference to the left-hand y-axis); the values are in 10^3m^2.

The temporal evolution of marsh area in C-C is given in Figure 35, as total marsh in both barriers (blue solid line), as marsh in Cacela (orange solid line) and in Cabanas (green solid line), as well as percentage of total marsh belonging to Cacela (orange dashed line) and Cabanas (green dashed line). Obviously, the summation of marsh areas of Cabanas and that of Cacela equals the total marsh in the subsystem and the summation of the related percentages for each year (dashed lines in Figure 35, with reference to the right-hand axis) equals 100%.
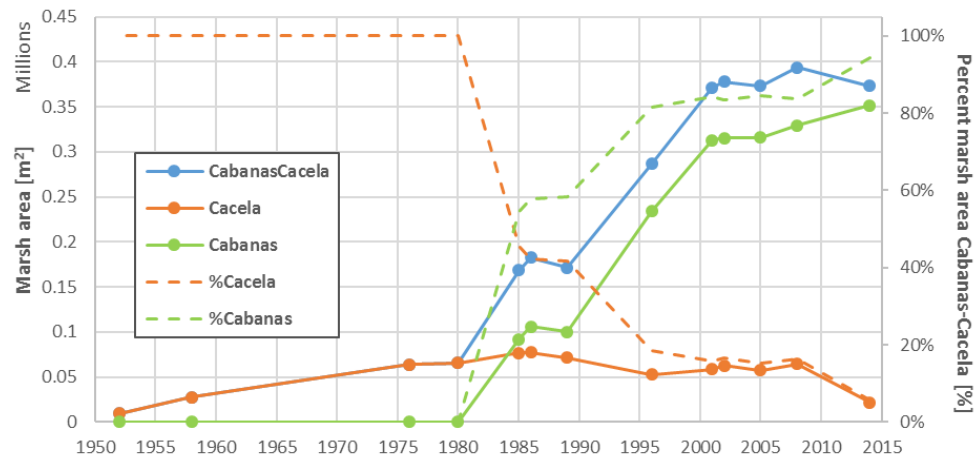
Figure 35: Evolution of marsh area in Cabanas and Cacela. The values for both barriers and for Cabanas and Cacela separately (in 10^3m^2 and with reference to the left-hand y-axis) and the percentages of total marsh pertaining to Cabanas and to Cacela (as dashed lines and with reference to the right-hand y-axis) are shown.
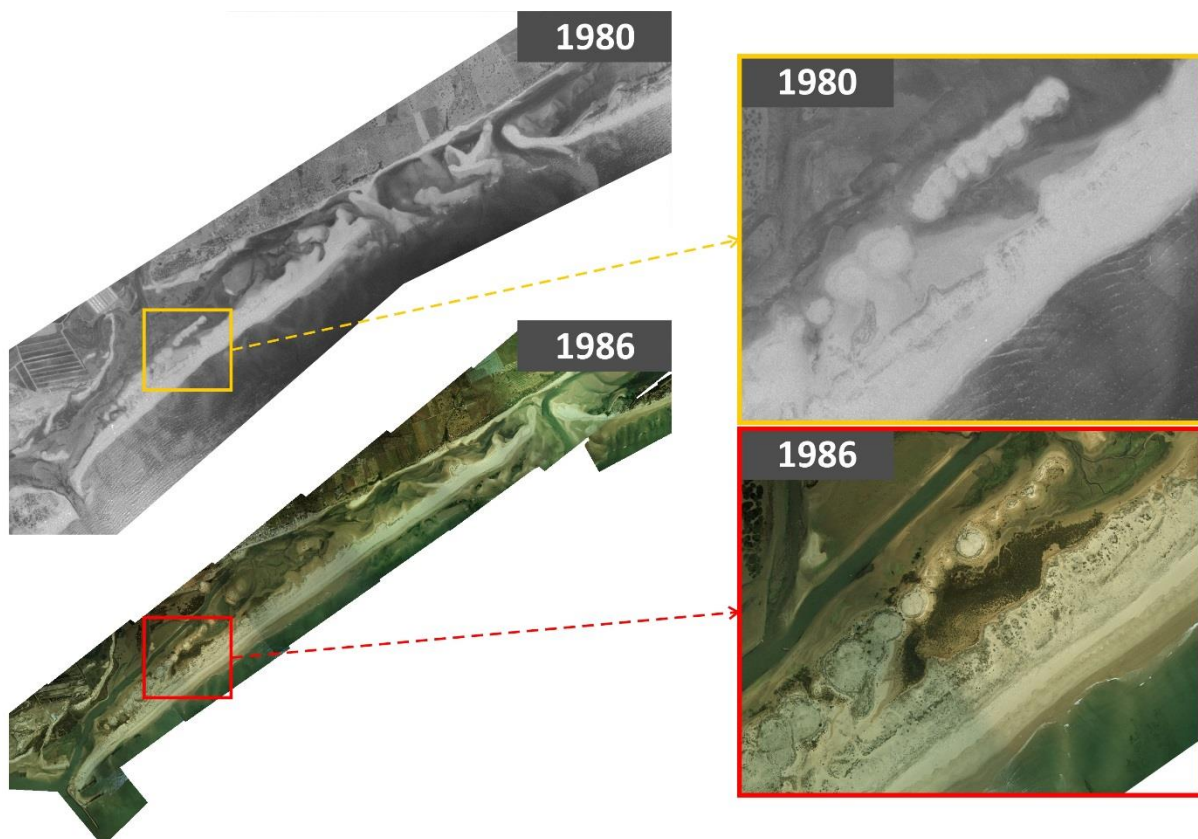
Figure 36: Aerial photos of Cabanas Island in 1980 and 1986 (and zoomed images to the right), showing areas of marsh growth, boosted by the disposal of dredged material that created an artificial embayment.

The data shows that initially, and until the early 1980s, the marshes are limited, perched to the Cacela Peninsula and were growing at a rate of $2 \cdot 10^3$ m²/yr. These marshes were confined in the eastern part, near the connection of the peninsula to the mainland. Following 1980, a boost in marsh growth is noted in Cabanas Island that lasts until the end of the study period, with a rate that is of the order of 10^4 m²/yr. This boost is, largely, due to the artificial formulation of enclosed embayments from disposal of dredged material in the western part of the lagoon. Figure 36 shows the marsh development in Cabanas between 1980 and 1986. These instances (magnified details of the images in Figure 36) show the absence of marsh and the enclosed bay, created by disposal of dredged material, in 1980 and the high development of marsh in the embayment in 1986. In total, the marsh development due to disposal of dredged material in Cabanas ranges from 50% of the total marsh in the barrier in 1986 to 35% in 2014. The remaining part of mash growth is highly related to the stability of the backbarrier of Cabanas after 1986 (shown in Figure 10 and Figure 11 and discussed in section 3.6.2) that provided favourable conditions for perched marsh development. In fact, the presence and growth of these marshes provide proof of the stability of the backbarrier environment of Cabanas Island from 1986 to present. Regarding the marshes in Cacela, they appear largely stable between 1986 and 2008 (Figure 35), with values that range within $5.3 \cdot 10^4$ m² and $7.7 \cdot 10^4$ m². In 2014 a significant reduction in marsh area is noted, with the values dropping to the levels of the 1950s (~$2 \cdot 10^4$ m²). This reduction is due to the eastward migration of the Lacém Inlet and the consequent shrinking of the peninsula (Figure 11).

5.2 Morphological Evolution Regimes

The main long-term barrier evolution trends for the period of 1952-2014, identified in Ria Formosa, are summed-up in Figure 37 and the related major evolution regimes and corresponding drivers of change (artificial triggers and natural mechanisms that sustain these regimes) are summarised in Table 3. Human pressures such as intense occupation (e.g. Ancão and Culatra) and frequent dredging of backbarrier channels (e.g. Ancão and Tavira) to ensure navigability are not considered in the analysis, since they generate changes at shorter spatial-temporal scales and can be omitted for the ones considered in the study.
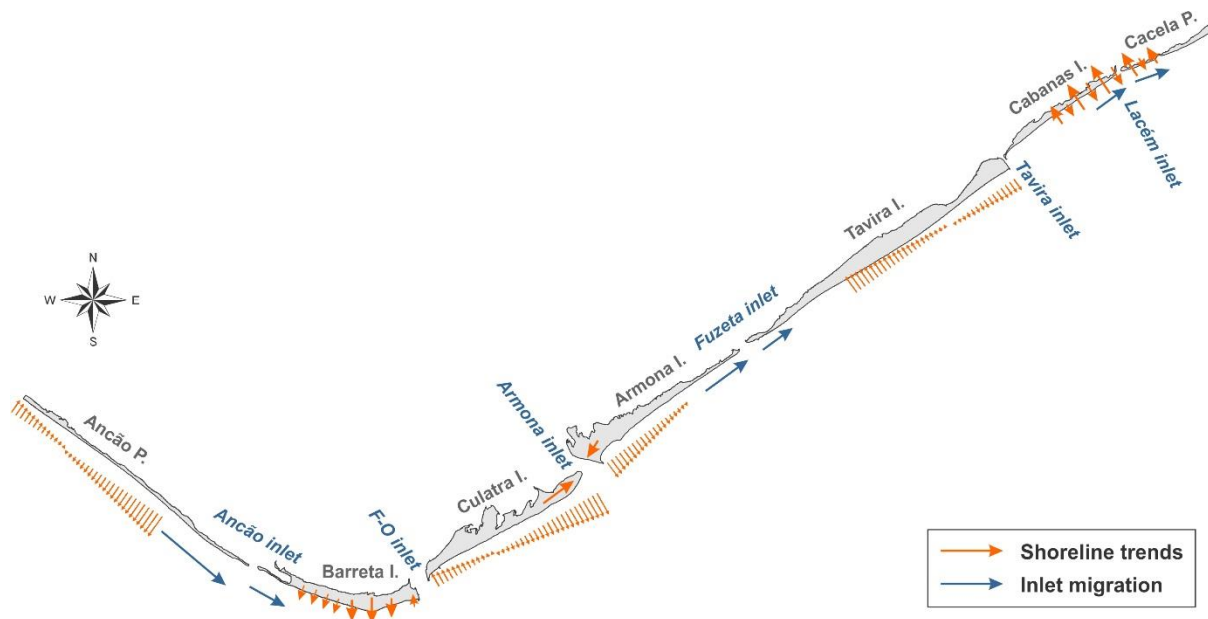

Figure 37: Schematic representation of the multi-decadal morphological response of the barriers of Ria Formosa. The major trends are noted as arrows (orange for shoreline and blue for Inlets) on the 2014 map.

Apart from the presence of the Vilamoura jetties, inlet relocations and beach-dune nourishments that are the main artificial factors in the area, the evolution of the Ancão Peninsula is largely dominated by longshore sediment transport, promoting its elongation and the eastward migration of the Ancão Inlet. The stabilisation of F-O Inlet played a decisive role to the evolution of Barreta, Culatra and Armona W, generally promoting growth in all cases (apart from localised erosion in Culatra directly downdrift from the jetty). For Barreta, it caused strong southward accretion by trapping sediments from longshore drift and by changing local circulation patterns around the western jetty. For Culatra and Armona W, the mechanism boosting this growth (and the narrowing of the in-between inlet) was the increase of the tidal flow through F-O and the corresponding loss of hydraulic efficiency in Armona after the stabilisation. Excluding the changes due to the eastward migration of Fuzeta, Armona E and Tavira W are relatively stable, supported by broad backbarrier zones. The stabilisation of the Tavira Inlet induced accumulation immediately updrift (east Tavira) and lack of sediment to the downdrift Cabanas Island, contributing to the generic erosive trend at C-C. Losses in W Cabanas are replenished using dredged matter (unrecorded), sustaining a 'forced' stability of the area. C-C have been at a transgressive state until 1986, fed by frequent overwash and the shallow depths of the backbarrier lagoon. From 1986 the barriers seem to recover, prograding seawards, passing on to barrier growth conditions. Overall, in the study period, C-C have been transgressing, while largely retaining the total barrier area.

Table 3. Morphological evolution of barriers, marsh maturity and related main artificial and natural drivers of change, triggering and/or supporting evolution (NR: Nourishment; LST: Longshore Sediment Transport; SBL: Shallow Backbarrier Lagoon).

Barrier		Evolution Regime		Marsh maturity	Limiting/Promoting Factors	
		Growth	Position		Artificial	Natural
Ancão		growing (SE)	stable	immature	Vilamoura jetties, NR	LST
Barreta		growing (S)	stable	mature	F-O jetties	LST
Culatra		growing (NE)	stable	immature	F-O jetties	Armona ebb shoals
Armona	W	growing (SW)	stable	mature	F-O jetties	Armona ebb shoals
	E	stable	stable	mature	-	broad backbarrier
Tavira		stable	stable	mature	Tavira jetties	broad backbarrier
C-C	up to 1986	reducing	retreating	immature	Tavira jetties, NR, dune NR with dredged material	SBL, overwashes, breaching, LST
	after 1986	growing	advancing	immature		
	over-all	stable	retreating	immature		

REFERENCES

Carrasco, A. R., Ferreira, Ó., Davidson, M., Matias, A., & Dias, J. A. (2008). An evolutionary categorisation model for backbarrier environments. *Marine Geology*, *251*(3–4), 156–166. https://doi.org/10.1016/j.margeo.2008.02.009

Dias, J. A., Ferreira, Ó., Matias, A., Vila-Concejo, A., & Sá-Pires, C. (2003). Evaluation of Soft Protection Techniques in Barrier Islands by Monitoring Programs: Case Studies from Ria Formosa (Algarve-Portugal). *Journal of Coastal Research*. Coastal Education & Research Foundation, Inc. https://doi.org/10.2307/40928755

Ferreira, Ó., Garcia, T., Matias, A., Taborda, R., & Dias, J. A. (2006). An integrated method for the determination of set-back lines for coastal erosion hazards on sandy shores. *Continental Shelf Research*, *26*(9), 1030–1044. https://doi.org/10.1016/J.CSR.2005.12.016

Ferreira, Ó., Matias, A., & Pacheco, A. (2016). The east coast of Algarve: A Barrier island dominated coast. *Thalassas*, *32*(2), 75–85. https://doi.org/10.1007/s41208-016-0010-1

Jabaloy-Sánchez, A., Lobo, F. J., Azor, A., Martín-Rosales, W., Pérez-Peña, J. V., Bárcenas, P., … Vázquez-Vílchez, M. (2014). Six thousand years of coastline evolution in the Guadalfeo deltaic system (southern Iberian Peninsula). *Geomorphology*, *206*, 374–391. https://doi.org/10.1016/j.geomorph.2013.08.037

Kombiadou, K., & Matias, A. (2017). *EVREST Project Report : Remote Sensing Database Report*. Faro, Portugal.

Matias, A., Ferreira, Ó., Vila-Concejo, A., Garcia, T., & Dias, J. A. (2008). Classification of washover dynamics in barrier islands. *Geomorphology*, *97*(3–4), 655–674. https://doi.org/10.1016/j.geomorph.2007.09.010

Morton, R. A., Miller, T. L., & Moore, L. J. (2004). National assessment of shoreline change: Part 1: Historical shoreline changes and associated coastal land loss along the US Gulf of Mexico. *U.S. Geological Survey Open-File Report 2004-1043*, 45.

Oliveira, S., Catalão, J., Ferreira, Ó., & Alveirinho Dias, J. M. (2008). Evaluation of Cliff Retreat and Beach Nourishment in Southern Portugal Using Photogrammetric Techniques. *Journal of Coastal Research*, *4*, 184–193. https://doi.org/10.2112/06-0781.1

Pacheco, A., Ferreira, Ó., Williams, J. J., Garel, E., Vila-Concejo, A., & Dias, J. A. (2010). Hydrodynamics and equilibrium of a multiple-inlet system. *Marine Geology*, *274*(1–4), 32–42. https://doi.org/10.1016/J.MARGEO.2010.03.003

Pacheco, A., Vila-Concejo, A., Ferreira, Ó., & Dias, J. A. (2008, January 10). Assessment of tidal inlet evolution and stability using sediment budget computations and hydraulic parameter analysis. *Marine Geology*. Elsevier. https://doi.org/10.1016/j.margeo.2007.07.003

Terrano, J. F., Flocks, J. G., & Smith, K. E. L. (2016). *Analysis of Shoreline and Geomorphic Change for Breton Island, Louisiana, from 1869 to 2014*. Virginia. https://doi.org/10.3133/ofr20161039

Thieler, E. R., Himmelstoss, E. A., Zichichi, J. L., & Ergul, A. (2009). *The Digital Shoreline Analysis System (DSAS) version 4.0—an ArcGIS Extension for Calculating Shoreline Change*.

Vila-Concejo, A., Matias, A., Ferreira, Ó., Duarte, C., & Dias, J. M. A. (2002). Recent Evolution of the Natural Inlets of a Barrier Island System in Southern Portugal. *Journal of Coastal Research*, *36*, 741–752.

Vila-Concejo, A., Matias, A., Pacheco, A., Ferreira, Ó., & Dias, J. A. (2006). Quantification of inlet-related hazards in barrier island systems. An example from the Ria Formosa (Portugal). *Continental Shelf Research*, *26*(9), 1045–1060. https://doi.org/10.1016/j.csr.2005.12.014